DARWIN Mission Summary Status

Reference	SCI/AM/DARWIN-SUMSTAT/06
Issue	2
Revision	2
date of issue	19th February 2007
Prepared by:	ESA-SciA

European Space Agency
Agence spatiale européenne

ESTEC

Keplerlaan 1 - NL 2201 AZ Noordwijk ZH - The Netherlands
Tel (31) - Fax (31) -

Table Of Contents

ESTEC
Keplerlaan 1 - NL 2201 AZ Noordwijk ZH - The Netherlands
Tel (31) - Fax (31) -

I INTRODUCTION

Darwin is one of the most challenging space projects ever considered by the European Space Agency. Its principal objectives are to detect Earth-like planets around nearby stars, to analyze the composition of their atmospheres and to assess their ability to sustain life as we know it. The Darwin mission is conceived as a nulling interferometer operating in L2 which makes use of on-axis destructive interferences to extinguish the stellar light while keeping the off-axis signal of the orbiting planet.

The objective of this document is to summarize the status of the activities related to Darwin that have been recently completed by ESA. Most activities have been performed under ESA contracts in European Industries and Scientific Institutes. These activities cover the development of core technologies, the design and manufacture of critical payload subsystems, tests of technology demonstration breadboards, the development of software simulators, studies of candidate Darwin payload and spacecraft architectures, and definitions of guidance, navigation and control systems for multi-spacecraft missions.

2. DARWIN SCIENCE STATUS

2.1 Scientific background

Exoplanets were discovered when first Latham et al. (1989) and then Mayor & Queloz (1995) and Butler & Marcy (1996) reported bodies of a mass less than 13 Jupiter masses (considered to be the dividing mass above which the object is a Brown Dwarf star). The continued work of these and other researchers have since then lead quickly to the understanding that bona fide exo-planets are to be discovered, and thus, the first steppingstone on the path to finding true 'exo-life' was taken.

The field of exo-planets has developed with remarkable speed. Currently (early 2007) we know of more than 200 planets in more than 140 exo-systems. What still eludes us is what has come to be regarded as the 'holy grail' of Life Detection outside the Solar System, namely 'true' Terrestrial (or 'rocky') planetary bodies like our own Earth found inside their star's so-called 'Habitable Zone'. The HZ is defined as the volume in space where water would be found in liquid form without postulating special conditions on the planetary surface, like e.g. a very strong greenhouse effect. A related definition is the Continuously Habitable Zone, where one also takes into account stellar evolution and the consequently changing of the luminosity of the central source. This therefore indicates the volume of space where life as we know it could arise and continue to exist during very long time periods.

Although we have found plenty of planetary systems around solar type stars in the vicinity of our Sun we have not found any indication of *systems* like our own, e.g. with giant planets in circular orbits *outside* the HZ. The discovery of such systems would at least allow for the possibility of terrestrial bodies being in the HZ although current technologies do not allow for their detection. This situation is of course at least partly caused by an observational bias. The ground based methods used so far – detection of the above mentioned radial velocity deflection caused in the stellar spectrum by a sub-stellar mass orbiting the primary, or the occultation of part of the stellar light when the planetary body passes between us and the star – has so far not had the sensitivity to either detect Earth-size objects, nor has the time been long enough to pick up planets similar to our Jupiter or Saturn (periods of 12 and 29 years). Progress is being made continuously, however, and objects with (minimum) masses of order 8-10 Earth masses are now being picked up with some regularity. Note that the masses of most planets detected so far are minimum masses since most of the methods used determine only one component of the velocity of the star (see below). Recently, however the technique of gravitational lensing has been successfully applied (e.g. Beaulieu et al, 2006). In a first detection of a possibly 'rocky' planet, a 5.5 Earth mass object ('absolute mass') has been detected orbiting some astronomical units away from a M-dwarf star that is itself located several kiloparsecs away from the Earth. Although there are several sources of uncertainties in this observation, it unambiguously shows the power of the method, and the ability to detect planets down to Earth mass. This makes it the prime candidate for first detection of worlds like our own. Nevertheless, this method also contains inherent uncertainties and will have to be used with care (see below).

While the ground based techniques that have hitherto been used continue to be developed, it has, however, recently become abundantly clear that to progress towards the direct detection and study of exoplanets the size of our own world will require instruments to be deployed in space.

The scientific rationale given for exo-planetary missions has been put into the broader context of the European Space Agency's (ESA) new science plan for the period 2015 – 2025. This plan – designated Cosmic Vision – divides the major scientific questions to be addressed by European space science during the next few decades into 4 themes, the first of which is "What are the conditions for Planet formation and the emergence of life?" Addressing the discovery and census of Terrestrial planets around nearby stars, as well as a first determination of their physical parameters – including their habitability is the challenging objective of Cosmic Vision theme 1.

2.2 The need to go to space

The prime methods that have been used so far (from the ground) are:

1. The radial velocity method
2. Occultation's of a star by a planetary body
3. Gravitational lensing
4. Astrometry

All of these methods have delivered tremendous results as can most clearly be seen from an inspection of *The Extrasolar Planets Encyclopaedia* web pages (http://exoplanets.eu) Nevertheless each method has severe limitations imposed by the measurements being conducted from the surface of the planet Earth.

The first method, the radial velocity method, measures the deflection of the spectral lines in a stellar spectrum, caused by the gravitational tug imposed upon its surface by an orbiting body. It is of course a function of both the mass of the orbiting body and its distance from the stellar surface, and therefore the method is naturally biased towards massive planets orbiting very close to the star, as pointed out by Struve in 1952. *It is interesting to notice that Struve also pointed out that there were no a priori reasons NOT to expect such planets, just because they are non-existent in our own Solar System.* As we want to detect planets like our own, we realize that an Earth-mass body, orbiting 1 astronomical unit away from a G2V (our Sun) star, will cause a deflection in the radial velocity curve of 0.1 m/s over a period of one year. This is significantly smaller than the amplitude change caused by the 5-minute acoustical oscillations in the solar atmosphere (so-called p-modes), the modes of which have life times of roughly half a year. We also have the noise introduced by the solar activity, which have amplitudes that are similar or larger. If we search for an Earth within the zone where we expect to find life, around smaller, less luminous, solar type stars (K-dwarf stars), the situation is alleviated as regards the first two of these problems (larger planetary amplitude, p-modes likely to have lifetimes rather different from the orbital period since the orbital period is shorter and p-modes have longer life-times) but not in the third area (activity) where it may be actually somewhat worse. Taken together with the technical difficulties, it is clear that, while not impossible, it will be very hard to detect an Earth analogue from the ground with this method. It will require dedicated large telescopes with long observing runs (years). Further, since we only measure one component (along the line of sight) of the velocity, the mass of the planet that we determine will be a *minimum* mass. Some other methods (see below), can, in exceptional cases, be used to determine the other component which therefore can lead to an exact mass (only depending on the estimate of the stellar mass).

The second method in importance (so far) is the occultation method, which has already delivered results in a number (currently, September 2006 about 10 stars) of cases. This is also a method that shows significant promise of being important in space based applications – see the CoRoT and Kepler mission descriptions below). Here we detect the drop in the luminosity of the star as the planet passes between us and the star, and draw conclusions about both star and planet from the shape of the light curve. The problem here is of course that it is also biased towards large planets orbiting very close to a (small) star – a situation not found in our own Solar system. A Jupiter-size planet passing between us and a solar type star will cause a drop in luminosity of about 1%, while an Earth size body only causes a drop of about 10^{-4}. Further, the occultation lasts for some hours, which means that the shorter the period (the first detected occultation by an exoplanet repeat every 3.5 days) the easier it is to detect it. Taking into account the random orientation of exoplanetary orbital planes, results in a 1-2 % chance of an occultation happening for planets close in, while it is significantly smaller for planets orbiting in the Habitable Zone of a solar type star. This means that this method needs to be applied either to very large samples of stars, simultaneously, or that one has very strong reasons to suspect that the planetary orbital plane is crossing the line of sight. This was the case for the first detected occultation – that of HD 209458b (Charbonneau et al, 2000). Using wide-field telescopes, either from the ground (where an additional limitation is the Earth's rotation which requires networks of telescopes) or from space, one can observe large numbers of stars at the same time. It is then a powerful method mostly limited by the disturbances in photometric precision induced by our atmosphere.

The advances that have been made through the detection of the gravitational lensing effect caused by large planets (and so far one case of a possible 'rocky' planet – Beaulieu et al, 2006) are very promising. This method is no-doubt going to be significantly developed during the next decade. It is a potentially very powerful method for determining statistics of exoplanets. The drawback is that for this method to work, one needs both a lensed object as well as a lensing system. In order to have any significant chance of detecting planets of all type, both sets of objects need to be large, which means that they will also be very distant. We then have difficulty assigning types and luminosities to both the lensed object and the lenser. The planetary mass will depend on both of these parameters. In the last case quoted above (Beaulieu et al, 2006), we assume that the blended image of the lensed object close to the galactic centre and the lenser at about half this distance are of F and M type respectively. We will not know this for many years as the star slowly moves out of the line of sight to the lensed object.

The fourth method, the astrometric method – where one measures the proper motion changes of a star as it travels across the sky, and interpret deviations from its predicted motion, is so far less successful. A number of multi-epoch observations carried out during the last century – mainly with long focus refractors – reported the discovery of large planets around some nearby stars. One can mention 70 Ophiuchi, where Reuyl and Holmberg (1943) found a 10 Jupiter mass body orbiting the star. None of these objects have been confirmed today.

Astrometric observations, utilizing mainly the fine guidance sensors on the Hubble Space telescope have been used to determine the deflection in the plane of the sky in a few cases. In the case of the planet Gliese 876b, the deflection is about 25 milli-arcseconds, which taken together with a well determine parallax leads to a planetary mass of 1.89±0.34 Jupiter masses, the largest uncertainty being the assumption about the stellar mass (Benedict et al, 2002). Dedicated space missions, with a capability of determining proper motions of a few micro-arcseconds, will make possible systematic surveys for planets of sizes down to maybe 10 Earth masses within the foreseeable future (see below).

Concerning the capability of Extremely Large Telescopes (ELT's) to directly detect exo-planets it should be noted that the problem here is to have a wave front arriving on the imaging detector of such a quality, that one can detect contrast differences of between 10^5 and 10^{10}. This should be possible within a distance from the optical centroid of the star that would be 0.5 arcseconds for Jupiter and 0.1 arcseconds for the Earth if viewed at a distance of 10 pc. The requirement that one needs to be able to detect the planet above the residual of the airy disk at these angular distances is daunting enough without adding the noise sources provided by the atmosphere and either the segmentation of very large telescope mirrors or in the case of monolithic mirrors irregularities in the mirror surface. Referring the reader to the paper by Chelli (2005), we can here only conclude that a telescope with 100m diameter, and with a correction of the wave front arriving on the detector to a precision 2-3 orders of magnitude better than what is currently achievable, is required to detect an Earth, orbiting in the HZ around an early G-type star. The limiting distance is for a search would then be 10pc (Chelli, 2005) to 18 pc (Gilmozzi). Within 18 pc we find a total of 39 single G-type stars (Kaltenegger et al, 2006). Further, most of these are found towards the later classes of the G types. All other solar type stars within the 18 pc limit will have their HZ at much smaller angular distances from the central object, and thus be significantly harder to detect. Add to this the problem that when searching for a planet similar to our own hosting life as we know it; the spectral signatures to search for are also in our atmosphere – only much stronger.

While thus not excluding the possibility of the detection of planets similar to our Earth from the ground, we may safely conclude that this is a very difficult task, technically at a par with the most complicated of space missions, but with a more limited scientific case.

2.3 The detection of life and spectral range

O_3 in the presence of liquid water is taken as a biomarker representative of the current Earth. Methane plays the same role in the history of the early Earth. There are strong features of these crucial substances found in the Earth's atmosphere at wavelengths near 12 µm (see Figures 2.1, 2.2 and 2.3). CO_2 at 15.8µm and O_3 at 9.3 µm are flanked by H_2O at 6.5 – 8 µm and beyond 18 – beyond 21 µm. Further CH_4 can be found at 7.5µm

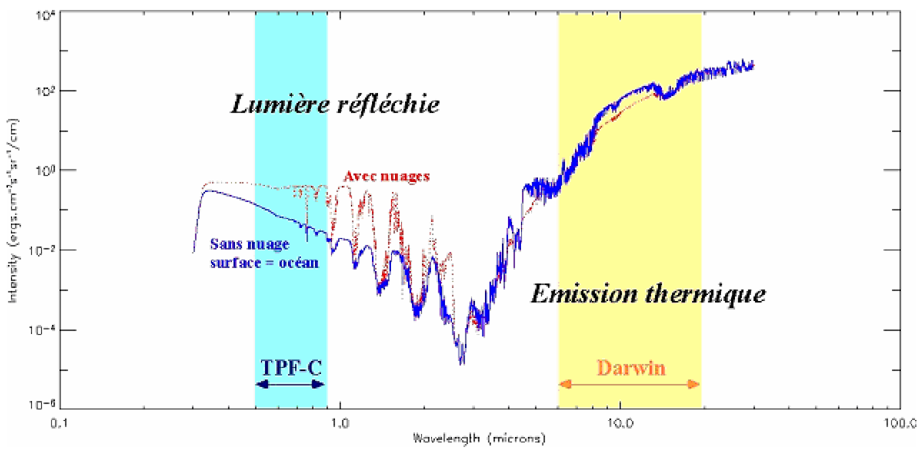

Figure 2.1: Model calculations (courtesy Franck Selsis) of the Earth's spectrum in two instances: With significant cloud coverage (red) and without cloud coverage (blue). The spectral ranges of ESA's Darwin and NASA's TPF-C are marked. Note saturation effect in the visible when the planet is cloud covered.

The spectral range that should be utilized is determined by two key factors:

1. The range where the contrast between the parental solar-type star and an exoplanet is the least. For an effective temperature of 300±50K for a planet, this is at ~ 12±6µm wavelength
2. Within the chosen range, signatures of the atmospheric composition and bio-markers must be found at relevant conditions (temperature, pressure, etc)

The requirement for the spectral range is thus that one must search for and measure the spectral signatures of O_3, CO_2, H_2O and ideally also methane CH_4. The required spectral range (in the infrared) would then be either 6.5 to 18 μm or 7.5 to 20(+) μm, and ideally 6.5 – 20(+) μm, since the H_2O may be better discerned at the low-λ end for more distant fainter, smaller stars, and better at the high-λ end for hotter stars.

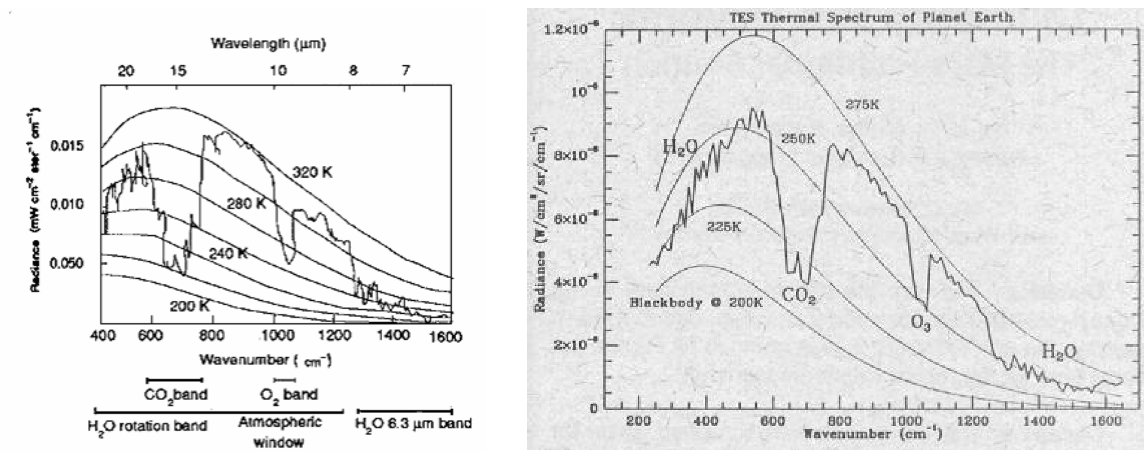

Figure 2.2: Earth spectra obtained with the Nimbus 4 satellite. *Left:* Spectrum taken towards the Sahara desert ('Desert planet'). *Right:* Spectrum obtained towards the Pacific ('Ocean planet'). Significant lower temperatures are obtained towards the Pacific. Also note the variation of black body temperature in different parts of the band.

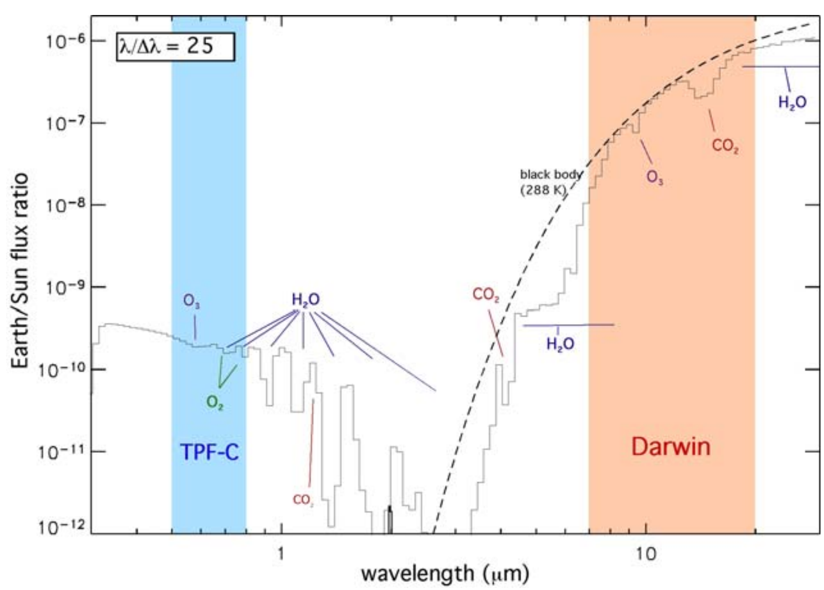

ESTEC
Keplerlaan 1 - NL 2201 AZ Noordwijk ZH - The Netherlands
Tel (31) - Fax (31) -

Figure 2.3: Model calculation made by Franck Selsis demonstrating the two spectral bands available to planet search missions and the spectral features available for planetary characterization. Note particularly in the IR, that one needs to measure the continuum centred at 12.6 microns to a high precision in order to evaluate if a) H_2O is present at either 6.5 μm or 20 μm; and b) how much H_2O is present.

A quick determination of physical conditions (and even the presence of an atmosphere) can be obtained already in a possible survey stage of a possible future space mission if we can measure relevant colours. Colour can distinguish different types of planets from each other, and from other objects such as structure in an exo-zodiacal cloud. Reference colours are those of the solar system planets in the relevant spectral band. We need to measure <u>at least</u> 3 colours (bands). These bands consist of two on the continuum below the CO_2 line at 15.5μm. With a third band centred on the CO_2 line, planets with atmospheres will be identified immediately. These colours can be established very rapidly through immediate post processing. The color bands should be:

1. Continuum 1: 8μm – 9.3μm
2. Continuum 2: 10.2μm – 13μm
3. Line 1: 13μm – 18μm

Note a fourth colour band could be 9.3 μm – 10.2 μm straddling the O_3 line.

2.4 High Level Scientific Requirements

As far as we can tell, from our limited statistics of one, and our (still) very poor understanding of what life really is and how it forms, we need a planetary surface in order to expect the processes that have apparently taken place on our planet. We then need to properly understand how planets form and evolve, and particularly how a Solar System like our own come to be, and why so many of the systems found so far external to our own look completely different. This means that we will have to understand the physical processes involved. In turn, this will compel us to fully understand, at least empirically, the birth, evolution and death of stars in more detail.

In Fridlund (2000), the high level scientific requirements were described in the context of space missions, as being the answer to the following questions:

- Are we alone in the Universe?
- How unique is the Earth as a planet?
- How unique is life in the Universe?

In order to answer these questions we then need to:

1. Search a large number of nearby stars for Terrestrial planets to find their frequency and location.

2. Detect planets within the so-called 'Habitable Zone'. In the early feasibility studies, the HZ was considered only in terms of black body temperature. No provision was made to take into account atmospheric pressure, etc
3. Determine the planets orbital characteristics (period, eccentricity, inclination etc.)
4. Observe the spectrum of the planet. Detect the presence of an atmosphere, and determine the effective temperature and diameter of planet (through the albedo).
5. Determine the composition of the atmosphere and the presence of bio-markers, viz. the presence of water and ozone/oxygen in an Earth type planet, mainly inert gases in a Mars/Venus type planet and Hydrogen/Methane atmospheres in Jupiter type planets or 'primordial' Earth-like planets

Any future space mission should therefore have the capability of detecting an Earth size planet with a representative temperature, orbiting a solar type star at a distance of 1 AU scaled with luminosity, with a signal to noise (in an individual observation) of at least 5, at a distance of 25pc.

Similarly, the mission must have the capability of determining if planets do ***not*** exist around a particular star and within the HZ with a high degree of confidence. This could require repeated observations since the location of the planet could in any instance be where it is unobservable (e.g. behind or in front of the star). Therefore, there should be at least a 90% confidence in a non-detection of Terrestrial planets in any given system after the mission.

The number of detected systems is a success parameter of the mission. One may argue that detecting ***one*** exo-Earth would at the time of the first such observation constitute at least a partial success. Nevertheless, the goal is to be able to draw conclusions about the origin of our Solar system, its evolutionary history, and its future development. This requires the number of detected systems to be at least one per evolutionary era (such an era is typically ~ 300 million years on the Earth) and ideally many more. A tentative number would be at least 15 systems that would need to be studied in detail. However in order to draw significant statistical conclusions a number at least a factor 3 higher is required. Hence, we can attempt to define one success parameter as:

Success parameter 1: In order to carry out the desired study of Earth-like worlds we should ideally detect a number of exo-planetary systems containing rocky planets in the habitable zone. This number should be at least 15 and ideally a factor 3 higher.

How many stars need to be observed in order to achieve this scientific requirement? In this context, there is also a need for a negative success parameter, since the possibility remains that the Earth is the only life-bearing planet or at least very rare in (our part of) the Galaxy. Our immediate neighbourhood, being located on the inside of one of the Galaxy’s spiral arms, consist of stars born very far away from their current location (the nearest star forming regions being 50

– 150 pc away). The stars that formed out of the same environment as the Sun are currently distributed across the entire Galaxy, and the chance of any of the target stars being formed together with the Sun is essentially nil. A negative success parameter therefore has to be defined in terms of how many stars need to be surveyed with a negative result for the result to be scientifically meaningful. This parameter then is defined as:

Success parameter 2: In order for a negative result (no terrestrial planets detected) to be meaningful, the mission need to survey at least 150 stars and preferably up to 300-500 stars (all solar type stars to 25 pc + M dwarfs) accessible to the mission with a 90% confidence that no terrestrial planet in the HZ has been missed.

These high level scientific requirements can be translated into specific observational requirements that can be converted into mission requirements. The process is detailed in Fridlund et al (2006), but can be summarized briefly as:

1. Ideally, the number of single, solar type (F - K main sequence) stars to be screened for Terrestrial exoplanets in their HZ during the primary mission is 387, which is essentially a complete sample of single F, G and K stars found out to 25 pc. M dwarfs, the most common stars in the Galaxy are also to be considered. The total number of known targets out to 25 pc is 628. Note detection is defined as obtained when the signal/noise ratio is least 5. The following ***minimum*** mission requirements can be established for the number of stars to be surveyed (incl. M dwarfs);
    a. 150, under the added condition that a significant amount of dust (10 times the level in the solar system) is present in every target.
    b. 225, under the condition of similar levels of dust as in the solar system.

2. Completeness of survey (probability that one has not missed a planet in the HZ for any given star) has to be better than 90%.

3. The presence of exo-zodiacal dust is considered to be an indication of the presence of a solar system, but will also hamper the detection of the planets. Therefore, the requirement is to obtain spectra for at least 10% of the surveyed systems (i.e. 15 in the case of high dust levels, and 22 in the case of solar dust levels).

4. Spectral signatures to be observed for each planet in any detected exo-planetary system – e.g. the so-called bio-markers CO_2, H_2O, CH_4, and O_3. The required spectral range (in the infrared) is therefore 6.5 – 20 μm, the required spectral resolution is at least 25 and the desired spectral resolution is 50 to also measure other gases. A feature can be considered to have been measured if its equivalent width has been determined to better than 20% accuracy.

We define a solar type star (at least in the present context) as being of the F5 – K9 main-sequence type, equivalent to a B-V colour index of $0.43 < B\text{-}V < 1.31$. These stars have main sequence time scales of between 2 and 20 Giga years, and any planet in the HZ would not have a rotation resonance, Stars later than K9 or so-called red or M dwarf stars are very different, in the sense that their energy output is extremely feeble. The HZ around such a star will be so close to the energy source that planets in it will suffer both from orbit – rotation resonance and ablation of the atmosphere by the stellar X-ray flux. M dwarfs are therefore ***not*** to be considered primary targets. On the other hand, that they require study because they may constitute a major component of the planet bearing energy sources in the Universe. The general scientific consensus is that 10% or less of the observing time should be spent on M dwarf observations.

The search space should overlap with the Habitable Zone in the target systems, i.e. where the black body temperature at 1 atmosphere pressure would allow H_2O to be in a liquid phase (see definition of HZ). Expressed in angular measure, this zone varies in distance and width for each stellar spectral type, according to the relation:

$$0.7\ \mathrm{AU} < r_{HZ}\,(L_{sun} / L)^{1/2} < 1.7\ \mathrm{AU}$$

The fraction of time for screening or spectroscopy spent on each stellar type should be distributed as follows: G: 50%; K: 30%; F: 10% and M: 10%. The observation times should be allocated in such a way that a maximum number of G and K stars can be surveyed.

The number of terrestrial planets existing in the galaxy is completely unknown at the present time. Hence the need to establish a second mission requirement regarding a negative answer (i.e. the *non-detection* of any Earth-like world) ought to be meaningful as well in a scientific sense. The excellent results obtained through radial velocity measurements have determined the prevalence of giant planets in orbits relatively close to solar type stars, in our part of the galaxy, to be between 5% (of all stars) and 15% (of high metallicity stars). Note that the determination of this number for terrestrial planets is one of the main objectives of the Corot and Kepler missions.

The position of the planet must be known with an accuracy allowing a determination of its orbit and the calculation of a good ephemeris. The orbit is also required so as to establish the planetary temperature. Orbital mechanics demand 3 observations in order to provide a good orbit. The separation of the instances of the observation can be calculated according to:

$$\Delta T = (365/6) \times (L/L_{sun}) \times (M/M_{sun})^{-1/2}$$

Here L_{sun} and M_{sun} are the solar values. The precision with which the position needs to be determined is 10^o with the goal of 3^o.

The precision with which we must measure the inclination, i, depends on the actual inclination (since cos i is the measured quantity). It will be 10^o for $i < 60^o$ and 20^o for $60^o < i$, 90^o.

One needs to determine a planets position with 10^{o} precision in the plane orthogonal to the interferometers pointing direction, at least 3 times separated by ΔT days. One also needs to determine the inclination of the system with a precision of 10^{o}. The planetary temperature should be known with a precision of 20 degrees K (desirable accuracy 10 degrees K) at 1 σ

Observations must be able to separate individual planets in the HZ in the case of multiple planetary systems.

2.5. The Input catalogue

An input catalogue for missions searching for terrestrial planets in the vicinity of the Sun has been prepared (Stankov, Kaltenegger et al, 2006). Based on available catalogues, most prominently the HIPPARCOS database, it is found that there are 1135 known objects within 25 pc. Faint (late type) K stars and red dwarfs (M stars) are known to be incomplete in this sample. Out of the 1135, about 500 are known to be double or multiple stars and are excluded, leading to a sample of 628. Of these about 200 are giant M-dwarfs. Further out of this sample 18 are known to host exo-planets of the gas giant or ’hot Jupiter’ kind. It is expected that before any direct detection mission flies, other missions such as ESA’s GAIA will have made the sample complete, and about 1000 single objects will be available.

DARWIN SYSTEM STUDIES STATUS

3.1 Mission requirements

The two objectives of the Darwin interferometry mission are:

i) to detect and characterize earth-like exo-planets, which could harbour earth-like life

ii) to perform high resolution imaging of celestial targets using the aperture synthesis technique.

The Darwin mission is conceived to be implemented on several collector spacecraft (CS) and on one beam-combining spacecraft (BCS). In all the considered architectures the CS are located at equal distances from the BCS. The relative phase and intensity of the beams coming from the individual collectors, forming the interferometer, is controlled by the beam combiner payload. When the light beams, collected by the individual collectors, are coherently combined, the stellar light interferes destructively, while the light from the exoplanet can interfere constructively. This technique, to suppress light by destructive interference, is called nulling interferometry, and forms the basis for the Darwin mission and exoplanet detection and characterization. The mission implementation presents several challenges, in particular in the areas of 1) high precision static and dynamical optical systems as required by nulling interferometry, 2) thermal control of the cryogenic payload, and 3) operation of a multi-spacecraft formation.

Major top-level requirements to the Darwin studies were:

- The Darwin interferometer shall operate in two distinct modes, namely:
  i) a nulling mode, where the interferometer is used in a nulling configuration for exo-planet detection and spectroscopy, and
  ii) an imaging mode, where the system operates as a synthetic aperture imager, using constructive beam combination.

- The formation shall be placed in an orbit around the second Lagrange point (L2) so as to take advantage of the low force environment acting on the constellation.

- It should be possible to launch all satellites of the formation, to the desired orbit, with two Soyuz-ST/Fregat launchers or alternatively with a single Ariane5 launcher.

- The Darwin interferometer shall be able to detect spectral absorption lines of water, ozone and carbon dioxide in the mid-infrared spectrum between 6.5 and 20 microns of Earth-like planets with effective temperatures down to 260 K, around nearby solar-type stars (F5 – K9) and M-dwarfs out to 25 pc.

ESTEC
Keplerlaan 1 - NL 2201 AZ Noordwijk ZH - The Netherlands
Tel (31) - Fax (31) -

- The interferometer shall during the nominal mission be able to search at least 225 of the stars listed in the Darwin catalogue for presence of exoplanets, assuming an exo-zodi level corresponding to that of the solar system. The interferometer shall during the nominal mission also be able to search at least 150 of the stars listed in the Darwin catalogue for presence of exoplanets, assuming an exo-zodi level corresponding to 10 times that of the solar system.

- It shall be possible to spectroscopically characterise at least 22 exo-planetary systems during the nominal mission lifetime, assuming an exo-zodi level corresponding to that of the solar system. It shall be possible to spectroscopically characterise at least 15 exo-planetary systems during the nominal mission lifetime, assuming an exo-zodi level corresponding to that of 10 times the solar system.

- The observation time during the detection and the characterization phase of the mission shall be allocated as follows G-stars about 50 %, K stars about 30%, F stars about 10% and M stars about 10%.

In 2005, two parallel assessment studies of the Darwin mission were initiated that aimed to establish two quite separate and distinctive candidate designs of the Darwin mission, including the payload, spacecraft and ground segment, that could fulfil the science mission requirements within given technical constraints imposed by the candidate launchers. Within the scope of these studies, Alcatel Alenia Space (AAS) and EADS Astrium Space (EAS) have evaluated the scientific requirements and derived the mission requirements, performed a trade-off among mission concepts and decided in agreement with the ESA to study the implementation of two nulling interferometer concepts:

- the three telescope nuller (TTN) concept with a BCS above the plane of the CS (the so called Emma concept) was studied by AAS,
- the X-array configuration with a co-planar BCS was studied by EAS.

3.2 Assessment study of a three telescopes nulling (TTN) space interferometer

The baseline concept studied by Alcatel-Alenia Space (AAS) is illustrated in Fig. 3.2.1. It consists of a free-flying configuration with three collector spacecrafts (CS), each carrying a 3.15 m diameter mirror, and a beam-combiner spacecraft (BCS) located above the plane of the collector spacecrafts (CS), the so-called Emma concept. The BCS is located 1200 m above the CS plane, allowing baselines of up to 168 m for nulling operation and 500 m for interferometric imaging. These limits are a trade-off between polarisation, thermal and straylight aspects.

The CS payload consists of a spherical mirror without a secondary mirror, allowing a simpler and more lightweight design, and simpler sun shield. Because the BCS should avoid pointing directly towards the Sun, the sky access is limited to an annulus around the anti-Sun vector, limited by an inner angle of 46°, and an outer angle of 83°. As the configuration moves with L2 around the sun during one year, eventually almost the entire sky is accessible. The TTN Emma concept has the advantages of almost maximum sky access for periods of up to 160 days per year for mid-latitude stars, allowing long spectroscopy integrations when necessary.

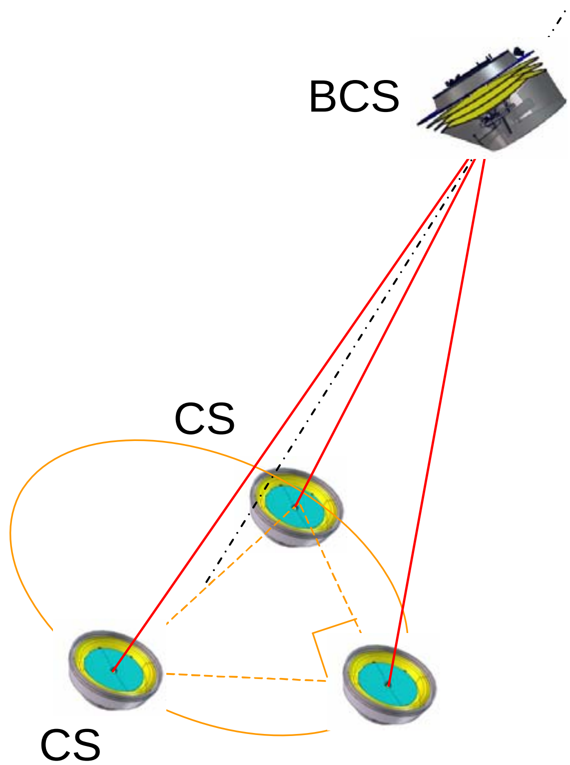

Figure 3.2.1: The DARWIN Orthogonal Three Telescope Nuller configuration, showing the distributed payload on the collector spacecraft (CS) and on the beam combiner spacecraft (BCS) in science mode formation flying.

The Three Telescope Nuller uses the minimum number of telescopes to obtain a θ^2 null for two simultaneous conjugate modulation states, allowing a maximum modulation efficiency for the planetary signal of 93.3%, while maintaining a relatively simple optical design. The design is based on either a classical modified Mach-Zender beam-combiner with co-axial beam injection, or a combination of a standard modified Mach-Zender beam combiner, and multi-beam injection into a single-mode fiber. In both cases an additional ~25% efficiency loss is unavoidable, either due to imperfect balancing of the combined beams, or additional coupling losses. The multi-beam injection may have the additional advantage of enhanced background rejection, but the multi-beam fiber injection is an order of magnitude more sensitive to beam tilt than co-axial beam injection, while the instability noise problem remains to be addressed for the TTN. This is the topic of an ongoing theoretical and experimental study.

Data collection is foreseen in continuous mode, although it remains to be seen whether polarization differences between the individual beams can be kept low enough over the full rotational cycle. The wavelength range is foreseen to be 6 − 20 μm. Three telescopes is the minimum number for internal modulation, necessary to filter competing signals from local and exo-zodiacal clouds, thermal radiation and leakage, which, in combination with the absence of secondary mirrors and small sunshield requirements, implies that a maximum collecting area can be realized within the mass envelope of the launcher. On the other hand, the straylight rejection on the BCS requires it to remain fixed with respect to the Sun, while the configuration of telescopes is slowly rotating, demanding complicated receive optics. For large baselines, the three beams arrive from noticeably different directions at the BCS, inducing non-zero polarization.

As the CS payload in the Emma configuration only contains a primary mirror, the overall payload volume on the CS is quite small (see Fig. 3.3.2) and the size of the CS in the Emma configuration is driven mainly by the mirror diameter.

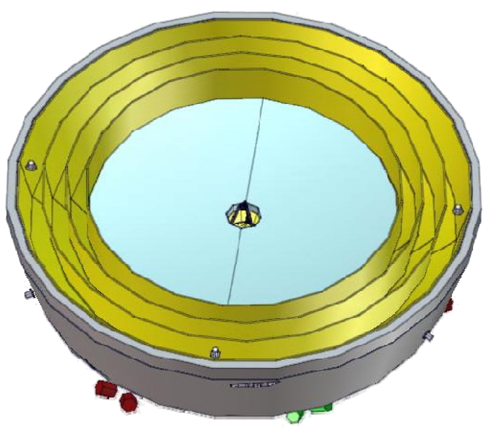

Figure 3.2.2: Collector spacecraft of the DARWIN Three Telescope Nuller configuration

In the Emma configuration, the BCS is located near the focal point of the reflected light of the different telescopes. The optical implementation of the TTN beam combination is performed in five stages (see Fig. 3.3.3):

1: the transfer optics + BCS/CS metrology stage that includes collimator and a scan tip-tilt mirror (derotator), a beam compressor and an inter-satellite optical metrology system,

2: the correction and modulation stage that includes an optical delay line and a fine tip-tilt mirror, a deformable mirror, wavefront sensors that measure piston and relative Z2 to Z11 wavefront errors, and a beam switching device,
3: the spectral separation stage, which splits the science band in 3 spectral channels for injection into single mode fibers,
4: the beams mixing and phase shifting stage,
5: the recombination, spectroscopy and detection stage.

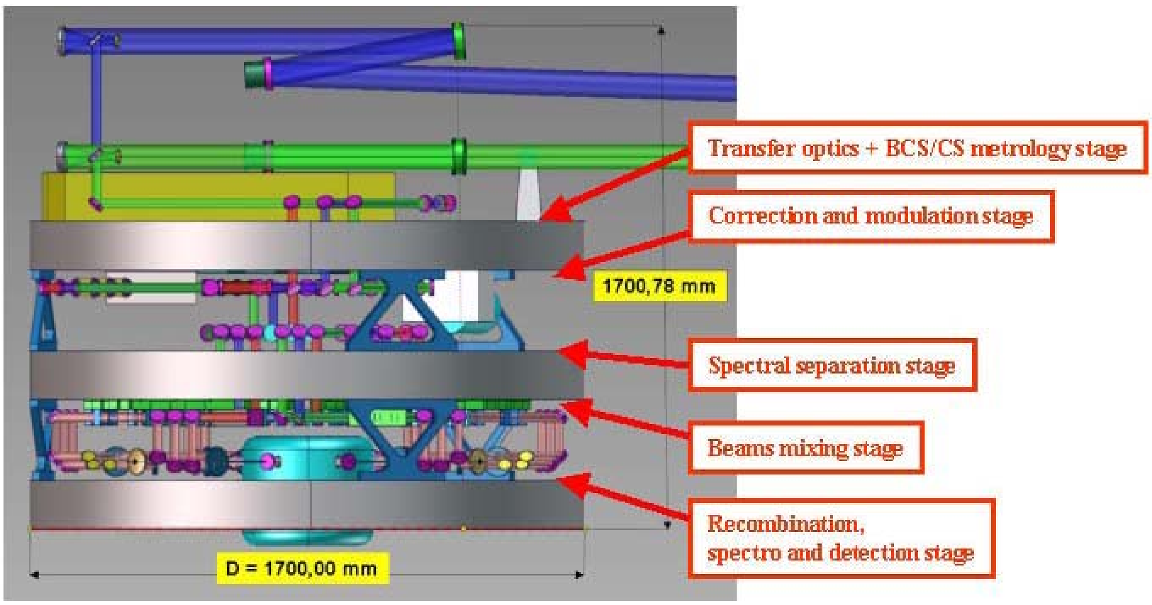

Figure 3.2.3: Optical assembly of the TTN BCS payload consisting of five different stages

The thermal design is based on passive thermal control to achieve cold temperatures for both BCS and CS. This implies extensive use of sunshields. Due to the small volume of the payload, the Emma configuration allows a simple fixed sunshield design. As a consequence, the baselines (measured between the centers of the primary mirrors) as short as 9 meters are possible. With the sunshield approach, the temperature of the optics is kept at about 40 °K. Sorption coolers are needed to provide low operation temperatures for the spectrometer optics and detectors. These sorption coolers are able to provide the required temperatures without exceeding the allowable levels of acoustic vibrations.

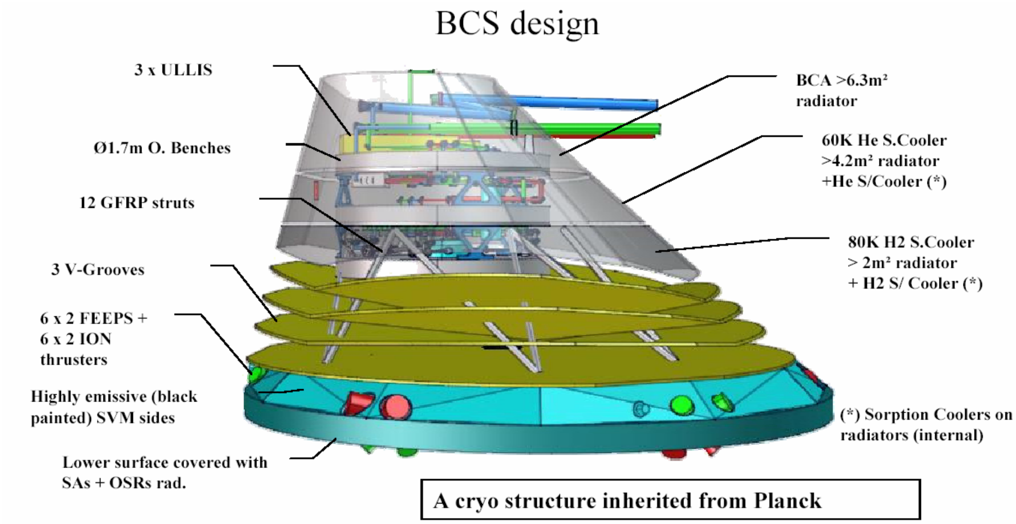

Figure 3.2.4: TTN beam Combiner Spacecraft.

The absence of secondary mirrors on the collector spacecrafts and the fact that only 3 collector spacecrafts are needed provide sufficient volume and mass margins for a launch on a single Ariane V ECA launcher. In this launch configuration, the four satellites are auto-stacked without the need for non-flight parts. The BCS is mounted on top of the 3 CS. The first CS is connected to the launcher through a classical ∅2624 mm clamp band interface as described in the Ariane V user's manual. On its upper part, the first CS provides a ∅4500 mm interface for the next CS which is mounted up side down with the same clamp band design. Interface frames are realized in titanium and connected by an external carbon fibre shell that provides the load path. The mass budget indicates that a TTN non-planar mission concept with ∅ 3.15m mirrors CS could be launched with an Ariane 5 ECA into a L2 orbit assuming some reasonable development effort in mirror light-weighting.

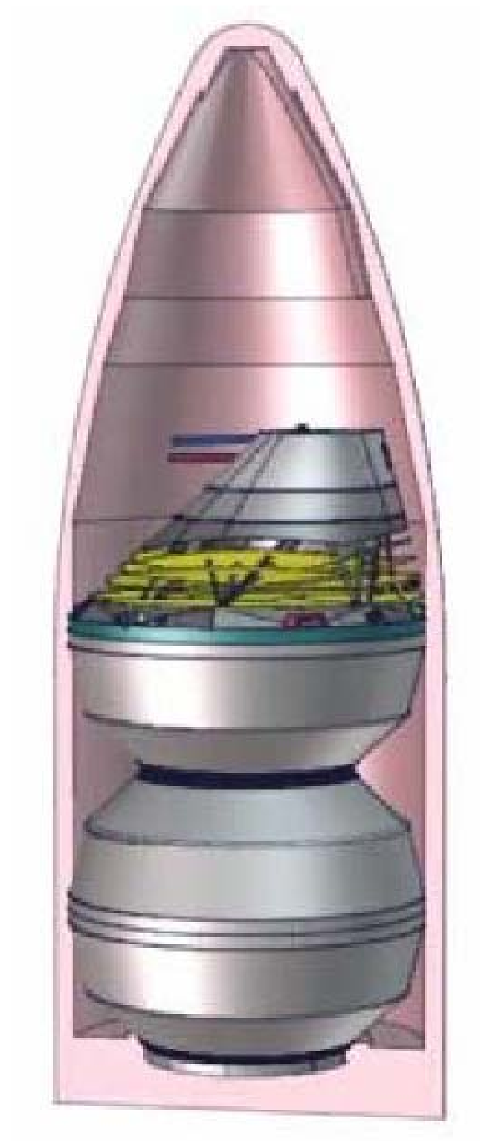

Figure 3.2.5: DARWIN TTN spacecraft stack, consisting of 3 collector spacecrafts and 1 beam combiner spacecraft (on top), accommodated within the Ariane 5 ECA launcher fairing. Such a accommodation provides a more than adequate system margin.

3.3 Assessment study of a four telescopes (X-array) nulling space interferometer

The baseline X-array concept proposed by EADS-Astrium is illustrated in Fig. 3.3.1. It consists of four collector spacecrafts and a beam-combiner spacecraft, all located in the same plane and forming an X-array configuration. Each spacecraft comprises a payload module , passively cooled to a temperature of 40 K by means of the sunshields, and a service module, operating at a temperature of about 300 K that provides the service functionality to the payload. The X-array consists of two single Bracewell θ^2 nullers along the short baselines, which are combined with a $\pm\frac{1}{2}\pi$ phase shift to provide two simultaneous modulation states. The long baseline provides the fine spaced modulation in the bright fringes, which allows planet detection with high angular resolution. In this way, the resolving power and nulling performance of the configuration are completely decoupled. This is a characteristic feature of the X-array family of configurations. In principle the resolution baseline can be made arbitrarily large, but in practice it is limited by straylight considerations. The range of CS to BCS distances is 15 to 300 m. An imaging to nulling baseline ratio of 3:1 has been selected as this allows for a good compromise between optimum scientific performance and instrument design constraints. In order to remove instability noise during post-processing, a 6:1 ratio is required (Lay, 2006).

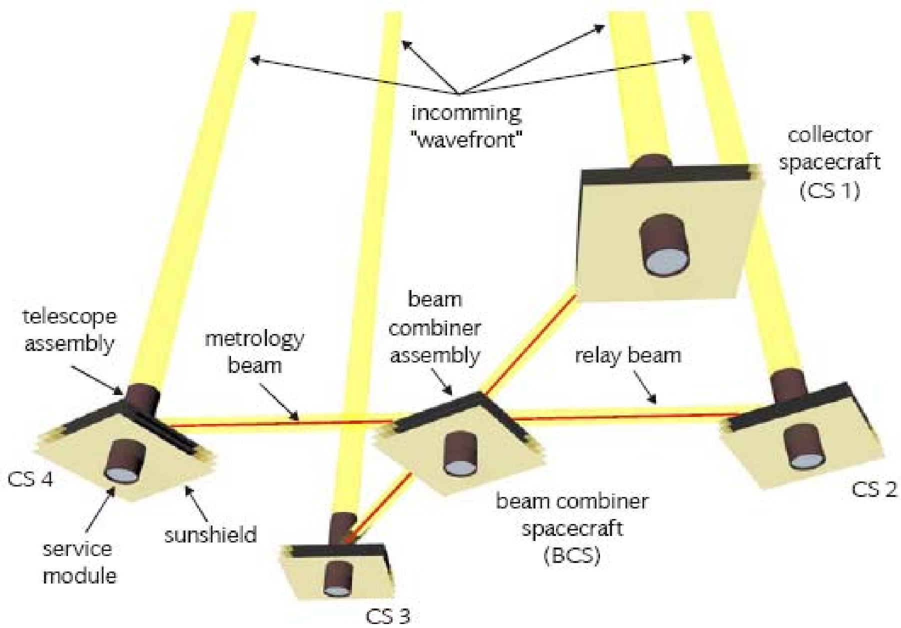

Figure 3.3.1: The DARWIN X-array interferometer configuration, showing the distributed payload on the collector spacecraft (CS) and on the beam combiner spacecraft (BCS) in science mode formation flying.

Major advantages of the x-array configuration are that only two-beam recombination stages are required which allow for a recombination efficiency of 100% and that the high-accuracy π phase shifter required for nulling can be realized by a perfectly achromatic periscope. The ±½π phase shifts, which are more difficult to set up accurately in an achromatic manner than π shifts, are applied only to the nulled outputs of the two Bracewell sub-interferometers. Hence small errors in these phases will not degrade the null, alleviating the requirements on the associated optical equipment.

The four collector spacecraft (see Fig 3.3.2) are designed to be almost identical. The payload design is driven by the requirement of highest stability and utmost symmetry between the beams to be recombined. For the collector telescope a Gregorian design has been assumed. To allow for compact stowing, a deployment mechanism is foreseen for the secondary mirror assembly support arm. The deployment arm is folded around the telescope during launch to allow for stacking of the spacecraft on top of each. The secondary mirror assembly is aligned after deployment by aid of an alignment mechanism and laser metrology. The size of the deployable sunshields limits the angle away from the anti-Sun vector over which the sky can be observed. This angle is 45°, which allows for a maxim of 90 days continuous observation time per year for stars in the plane of the ecliptic.

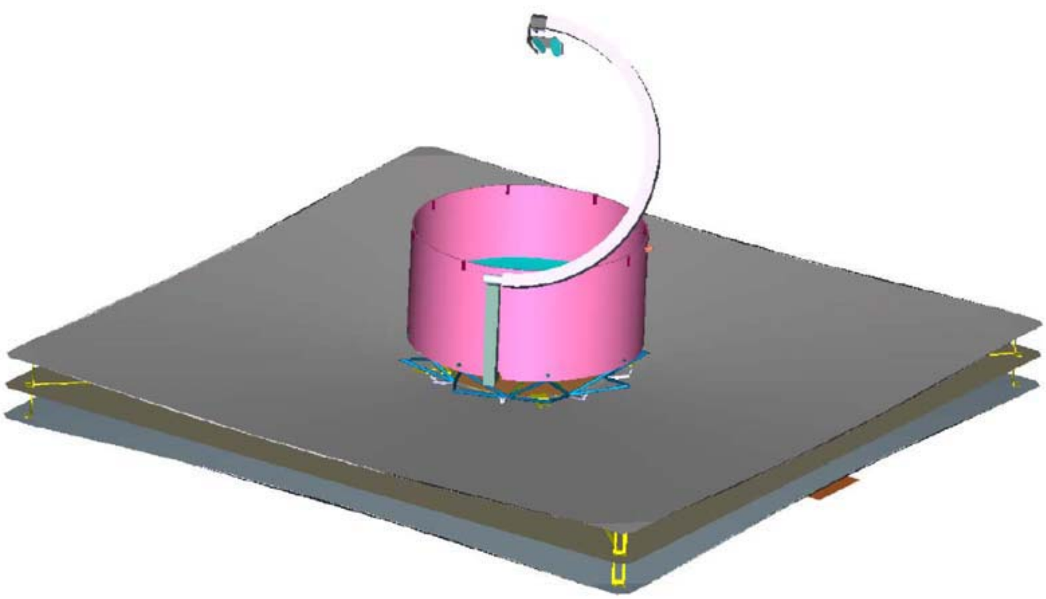

Figure 3.3.2: The DARWIN X-array collector spacecraft (CS) in deployed configuration.

The incoming wave-fronts received by the collector telescopes mounted at the CS are relayed by folding mirrors to the BCS. The 200 mm diameter relay beams are compressed to 10 mm by relay telescopes at the BCS. After fine-pointing and disturbance control, including OPD and intensity control, the beams originating from the individual spacecraft are equalized to a sufficiently high degree. The optical assembly of the BCS payload comprises 3 optical sub-assemblies (Fig. 3.3.3), the receiver optical assembly, the nulling optical assembly and the detection optical assembly. The nulling optical assembly consists of the nuller itself, a phase modulator for phase chopping, and a recombiner. The nuller and the recombiner are realized in bulk optics. Wavefront filtering is achieved by the co-axial injection of single beams into separate single mode fibres, which convey the signal to the entrance slit of a spectrometer consisting of a collimator, a disperser and a camera. The detector assembly is included in a separate compartment which is actively cooled to a temperature of 6 – 8 K. The detector output signals are processed by the instrument control and the science data is transferred to the on-board computer. The instrument control also interacts with the disturbance control and the formation control.

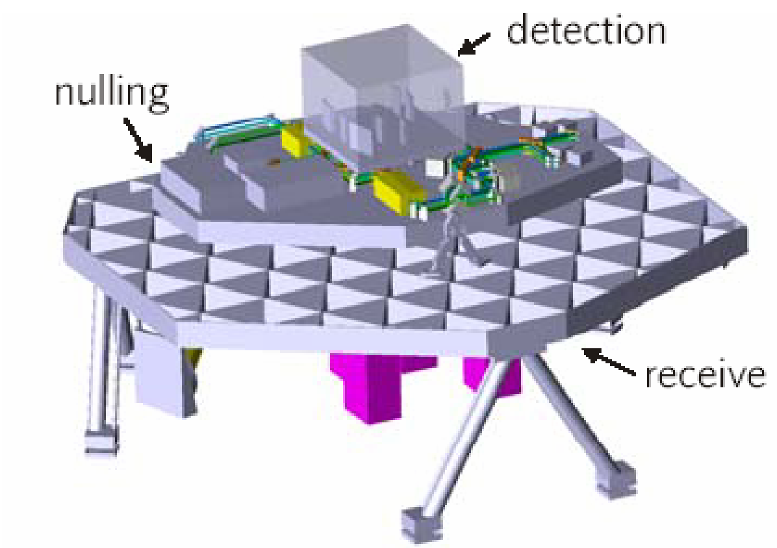

Figure 3.3.3: Optical assembly of the BCS payload consisting of the receiver optical assembly (lower level), the nulling optical assembly (intermediate level) and the detection optical assembly (upper level).

The formation control functionality is distributed among the payloads and service modules of all spacecraft. This has to do with the sequential modes of operation and the nested control architecture. The constellation envelope is established by the RF metrology, the precise formation by laser metrology and co-phasing is achieved by pointing and phase piston sensing with active optics. For constellation deployment when the payload is still switched off, the absolute attitudes (sun avoidance), relative attitudes, positions and velocities are sensed by equipment residing in the service module, namely the star trackers and the RF metrology. Once the constellation is established, the payload is activated and the precision pointing and formation flying can commence. The formation flying laser metrology is used as the sensor for precision lateral, longitudinal and relative attitude establishment of the constellation as required in the science mode. For science mode acquisition, this part of the optical metrology together with a precision pointing sensing will prepare the acquisition of coherent signatures from the source itself (fringes) by minimizing the search envelope. For establishing and maintaining the interferometer co-phasing, the formation control relies crucially on information drawn from the science beams in terms of phase delay and precision pointing. In addition, the precise piston and tilt actuation on the science beams is accomplished by active optical actuators in the payload.

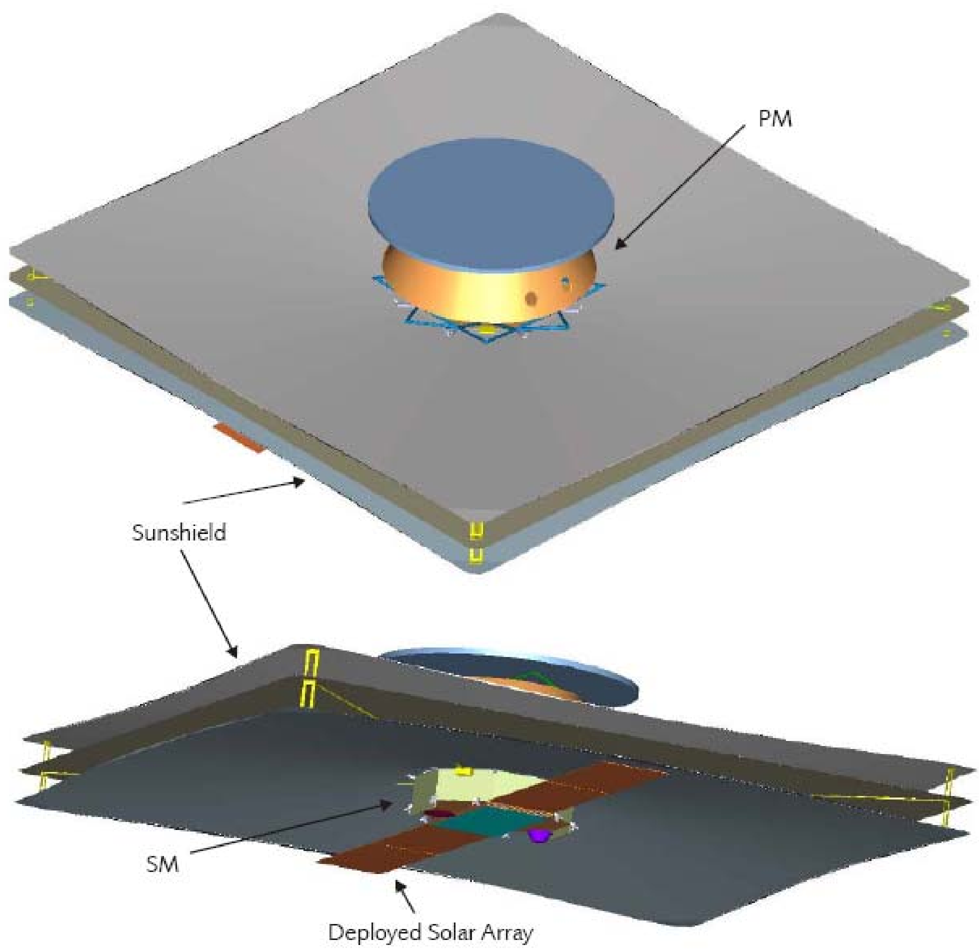

Figure 3.3.4: X-array Beam Combiner Spacecraft in deployed configuration.

Within the fairing of the Ariane V launcher, the beam combiner spacecraft is mounted on top of the spacecraft stack with the 4 collector spacecrafts stacked below. A special-purpose adaptor provides the interface to the 2624 mm diameter ACU mounting plane of the Ariane 5 ECA launch vehicle, see Fig. 3.3.4. Each collector spacecraft incorporates an outer cylinder that provides a primary load path from the top to the bottom of the stack outside of the diameter of the collector telescope main mirror. To allow for identical collector spacecraft, the stacking cylinders are identical and dimensioned for the bottom spacecraft. To limit the overall height of the launch stack, the height of each cylinder is sufficient to permit the service module of the upper spacecraft in its stowed configuration to be nested inside the cylinder of the lower spacecraft. The BCS is mounted on top of the stack via a support cone. The lower diameter of the cone provides the interface to the uppermost CS. The height of the cone is driven by the need for the optical beams from the CS to clear the edge of the deployed sunshield. The mass budget indicates that an X-array planar mission concept with ∅ 2.45m primary mirrors CS could be launched with an Ariane 5 ECA into an L2 orbit assuming some development effort in mirror light-weighting.

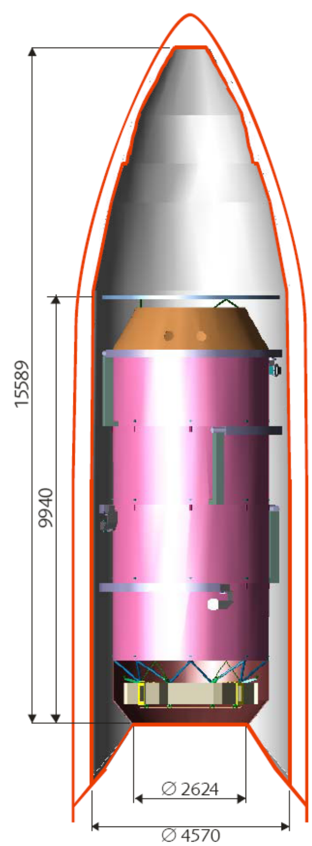

Figure 3.3.4: DARWIN X-array spacecraft stack, consisting of 4 collector spacecraft and 1 beam combiner spacecraft (on top), accommodated within the Ariane 5 ECA launcher fairing.

3.4 Preliminary comparison between the TTN and X-array space interferometers

The main differences between the studied TTN and X-array concepts can be summarized as follows:

- The number of CS and the resulting impact on launch mass and volume, and related to that, collecting area.
- The spacecraft configuration, with a BCS in plane with the CS for the X-array and a non-planar BCS for the TTN, It is important to realize that the TTN can be realized in a planar configuration as well as the X-array in a non-planar Emma configuration.
- The beam-combination principle, based on a modified Mach-Zender beam combiner, in bulk optics and with co-axial beam injection into the SMW for the X-array, and a combination of MMZ and multi-beam injection on the TTN. Again it is important to point out that it is possible to realize an X-array in a multi-axial beam-combination (MABC) set-up, as well as a TTN in a set of conventional MMZ beam combiners.

A list of major components and subsystems used in the payload module (PLM) and service module (SVM) of the beam combiner spacecraft (BCS) and of the collector spacecraft are given in Table 3.4.1 and Table 3.4.2, respectively.

3.4.1 Three vs. four telescopes

The optical design concept of the 4-telescope X-array configuration is (relatively) simpler since it does not need a beam derotator or an active mirror and makes uses of periscope π phase shifters that are inherently achromatic. Only low-accuracy dispersive phase shifters are needed in the X-array beam combiner optics since the phase modulation is done after nulling. It allows a maximum modulation efficiency of 100%. On the other hand, a fourth CS brings an extra service module (SVM), and thus has an impact on the payload mass. With an assumed 25 kg/m^2 telescope technology and a launch on an Ariane 5 ECA, the effective total collecting area drops from 21.2 m^2 for three CS to 15.2 m^2 for four CS.

The Three Telescope Nuller design is more complicated, in that it is based on 120° achromatic phase shifts, which require sophisticated combinations of coatings. The maximum modulation efficiency is limited to 93.9%. The beam combination can be realized either with conventional MMZ beam combiners and co-axial beam injection into multiple SMW, or multi-axial beam injection into a single SMW. In both these cases an additional 25% loss in efficiency is encountered, either because of unbalanced input beams, or additional coupling losses. The MABC scheme is claimed to have enhanced background rejection properties, which would boost the science performance, but this feature has still to be verified experimentally. MABC is an order of magnitude more susceptible to beam tilt at injection, whereas co-axial injection is an order of magnitude more sensitive to defocus and spherical aberration. A comparison of the main components in the payload module (PLM) of the BCS is made in Table 3.4.1.

From a science performance point of view, the X-array offers three advantages:

- A maximum modulation efficiency of 100%.
- Separation between nulling and imaging baselines, which allows a better resolution of multiple planets.
- A stretched version of the X-array (with a 6:1 or higher ratio between imaging and nulling baseline) offers a post-processing solution for the instability noise problem (Lay, 2006).

BCS	X-array planar	TTN non-planar
PLM	- 2 Periscope APS - 2 low accuracy APS - 2 MMZ, 4 ODL - Co-axial fiber injection - Monomode fibers - 2 spectral channels (late split)	- **CS configuration derotator** - 6 Accurate Dispersive APS - 3 MMZ, 3 ODL - Multi-axial fiber injection **(TBC)** - Monomode fibers - 3 spectral channels (early split)
SVM	- **deployable sunshield** - **deployable solar array** - phased array antenna - 3 propulsion systems	- fixed sunshield - fixed solar array - phased array antenna - 3 propulsion systems

Table 3.4.1: A comparison list of major components and subsystems used in the payload module (PLM) and service module (SVM) of the beam combiner spacecraft (BCS). Subsystems regarded as complex are marked in boldface.

CS	X-array planar	TTN non-planar
PLM	- ∅ 2.2 – 2.45 m primary mirror (Ariane 5 ECA) - **deployable M1-M2 arm** - **M2 mounted on a 5dof mechanism** - M1-M2 in-orbit alignment (metrology)	- ∅ 3.0 m primary mirror (Ariane 5 ECA) - no M2
SVM	- **deployable sunshield** - **deployable solar array** - phased array antenna - 3 propulsion systems	- fixed sunshield - fixed solar array - phased array antenna - 3 propulsion systems

European Space Agency
Agence spatiale européenne

ESTEC
Keplerlaan 1 - NL 2201 AZ Noordwijk ZH - The Netherlands
Tel (31) - Fax (31) -

Table 3.4.2: Compared list of major components and subsystems used in the payload module (PLM) and service module (SVM) of the collector spacecraft (CS). The subsystems regarded as complex are marked in boldface.

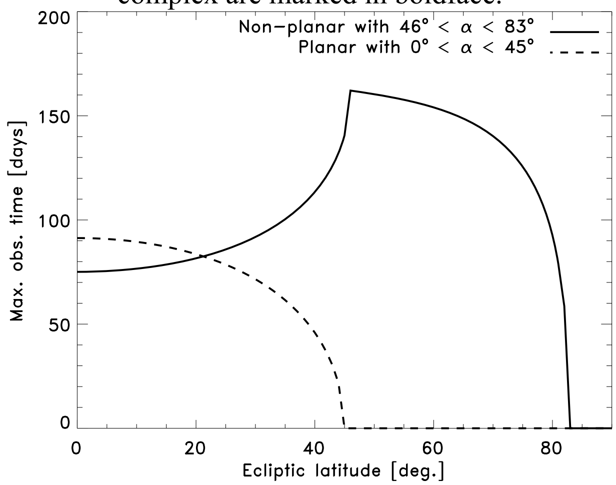

Figure 3.4.1: Sky access measured in terms of the maximum number of days per year a target can be observed as a function of ecliptic latitude of the target, for the non-planar (Emma TTN) and planar (X-array) configuration. The angle α is the instantaneous angle between the anti-Sun vector at L2 and the target position.

3.4.2 Planar vs. non-planar configuration

The choice between a planar and a non-planar configuration has important consequences for the PLM and the SVM on the spacecraft and the science performance.

- The CS PLM in the non-planar configuration design is simpler since it only consists of a single mirror. No mechanisms are needed for a secondary mirror deployment and in-orbit alignment as for the X-array.

- The BCS and CS SVM architecture is also simpler in the non-planar configuration, because the absence of an M2 allows the sunshields to be dimensioned smaller, such that deployment mechanisms for sunshields and solar arrays are no longer necessary. The absence of such deployable subsystems reduce the cost associated to testing, the risk associated to the number of mechanisms which have to be successfully deployed before the system gets operational, and the level of disturbances that can be amplified by deployed structures during operation.

- On the other hand, the planar design allows a simpler BCS PLM, based on a static optical relay between CS and BCS. In the non-planar configuration, the BCS has to remain fixed relative to the Sun, whereas the CS configuration is rotating, implying the need for more complicated receive optics, including a configuration derotator, on the BCS PLM.

- Smaller sunshields on the spacecraft in the non-planar configuration imply that smaller baselines are possible, which result in lower stellar leakage rates on stars with relatively large diameters (such as nearby G-type stars). On the other hand, the non-planar configuration does not allow a 100% compensation of differential polarisation between the (converging) input beams. As a consequence, there are strong limitations on the angular separation between the CS as seen from the BCS receive optics, limiting the maximum baseline to 168 m. This means that the non-planar are less suited for more distant systems,

- A non-planar design allows access to ecliptic latitudes between −83° and +83°, allowing 99.25% of the sky to be surveyed, rather than 70.7% as with the planar design. Not only are more (nearby) sources accessible, the times during which they can be observed during the year are also longer, as is shown in Fig. 3.4.1.

3.4.3 Comparison of science performance

In order to compare the science performances of the studied X-array planar and TTN non-planar configurations, simulations were performed with DarwinSIM (see section 4.4.1) with the following assumptions:

- The two mission concepts are to be launched with an Ariane 5 ECA into L2, and the collecting area is dimensioned accordingly.
- Each of the 628 stars of the Darwin catalogue is a possible target; 10% of these stars are assumed to have one Earth-like planet in their habitable zone, at six possible positions with equal statistical weight in the set of random positions on circular orbits with arbitrary inclination;
- Each star is surrounded by an exo-zodiacal dust disk identical to the solar zodiacal disk;
- 10% of the available observation time is spent on F stars, 50% on G stars, 30% on K stars and 10% on M stars;
- The integration times during the survey phase are dimensioned such that they allow the detection of an Earth-like planet at a signal-to-noise ratio of 5 in 90% of the possible positions inside the HZ around each target.
- The integration times required for spectroscopy are based on the establishment of the presence of the bio-marker absorption features O_3, CO_2 and H_2O with a SNR of 5 in an Earth-like spectrum. For the two continuum bands, which allow the establishment of the planetary blackbody background, a SNR of 30 is required.
- Spectroscopy is assumed to be done in a mode of continuous rotation, i.e., the spectrum is built up from repeated detection of the target system, and the planet signal is modulated during the spectrum acquisition. Although it would be more economic to perform spectroscopy in staring mode, where the planet is kept at a maximum of the transmission map during the entire spectrum acquisition, it is presently unknown if this mode of spectroscopy is feasible. Since

the planetary signal is no longer modulated noise excursions at all frequencies add to the total noise, requiring noise control over the full bandwidth, leading to very demanding requirements (see e.g. Chazelas et al., 2006).

The simulations did not take into account the effect of instability noise or any imperfection due to the actual engineering implementation. Neither were any effects due to the data reduction pipeline taken into account. The results of the simulations presented in Table 3.4.3 are therefore considered only as comparative and at best a rough approximate indication of the absolute performance.

Remarkably, the X-array planar and orthogonal TTN non-planar mission concepts have similar performances. This can be explained by the fact that (i) the better sky access of the non-planar TTN (and therefore the access to easier targets), (ii) the larger telescope diameters of the TTN that can be accommodated in an Ariane 5 launcher, and (iii) the smaller sunshields of the TTN (that enable smaller baseline specially for nearby stars) compensate the intrinsic advantages of the X-array concept. For the TTN non-planar configuration the 'classical' beam-combiner approach has been chosen based on MMZ and co-axial injection. If the experiments on MABC confirm a positive effect on the background rejection, the numbers in Table 3.4.3 may improve.

	X-array planar	**O-TTN non-planar**
	4 x 2.45 m collector mirrors (co-axial injection)	3 x 3.15m collector mirrors (co-axial injection)
# targets screened in 5 yrs	439	467
# targets screened in 2 yrs	339	314
# Spectra w/o H_2O spectro. G type star only:	20 4	18 4
# Spectra with H_2O spectro. G type star only:	12 0	9 1

Table 3.4.3: Compared performance of the X-array and the TTN non-planar concepts in term of number of stars detected or on which spectroscopy can be successfully conducted.

In summary, the X-array planar configuration has some inherent advantages and is presently a more mature nulling configuration. It provides a higher spatial resolution useful to disentangle multiple planet signals and the post-processing of the X-array data allows a partial removal of the instability noise by using a stretched imaging baseline. This has the potential for relaxed requirements on OPD and intensity control accuracy that are very difficult to achieve. Simpler optical engineering solutions are possible for the implementation of the beam combination scheme that does not need a de-rotating optics. The symmetry of the X-array optical scheme is kept during rotation which prevents any residual signal modulation due to polarization.

Nevertheless, for an Ariane 5 launch in L2, the orthogonal-TTN non-planar architecture is an attractive alternative since it has the potential for similar science performance with only three collector spacecrafts. The non-planar TTN concept enables a simpler spacecraft engineering solution without deployable sunshields, or deployable solar arrays. This avoids the risks associated with the large number of mechanisms that are needed in the planar X-array concept. This reduces the complexity associated with deployment mechanisms, e.g. regarding their testing and space qualification. It also minimizes the amplification of disturbances that could result from extended 'floppy' structures. The payload design of the collector spacecrafts is also simpler and avoids the risks and complexity associated with M1-M2 deployable arms and M2 alignment mechanisms. However, the sensitivity of the TTN concept to instability noise has still to be assessed. Both X-array and TNN architectures require a significant technology development effort in components (e.g. IR mono-mode fibers), subsystems and engineering breadboards.

3.4.4 Instability noise status

It has been realized that the noise spectrum of the phase and/or intensity perturbations have a strong impact on the stability of the null (Lay 2004). This so-called instability noise arises on the low-frequency side of the frequency spectrum, at the harmonics of the rotation frequency at which the planetary signal is modulated. Slow excursions of the null that are not removed by the internal modulation process end up in the detected outputs as fake planetary signals. Since the entire configuration is controlled by three layers of closed loop systems, from formation flying down to actuators on the BCS PLM, it is a reasonable assumption that in first approximation the residual noise fluctuations on phase and amplitude that contribute to the instability noise will have a white noise spectrum, or even a positive power-law slope at low frequency if Kalman or predictive filtering techniques are applied.

However, the sensors used in the control loops may be prone to drifts, which generally are assumed to have a 1/f spectrum at lower frequencies. These drifts will not be detected, as they are inside the control loop, i.e. they are drifts of the control loop zero point setting. Fortunately, the high requirements on phase and amplitude stability pertain only in a relative way, that is, between arms of the interferometer. The absolute phase may drift, as long as the phase differences between the arms of the interferometer is stable at the sub-nm level. Hence a beam switchyard in the BCS PLM, that permutates the arms with respect to the final control loop stages, will allow the removal of any low-frequency drift, as long as the drift excursions are constant during the permutation cycle of the beams. Hence, careful engineering will necessarily play an important role in the suppression of the instability noise problem.

Apart from engineering solutions, several post-processing solutions have been identified:

- One feasible solution has been found by Lay (2006). It requires a ‘stretched’ X-array (i.e. with an aspect ratio of 6:1 or higher), and a spectral resolution of 120 elements over the range 6 − 20 μm. Unfortunately, this solution relies on the separation between nulling and imaging baselines and is therefore not applicable to the TTN configuration. Due to the large aspect ratio it is also less compatible with a non-planar configuration.
- Lane et al. (2006) have proposed a method for calibrating the null, thus ensuring the low-frequency stability. In their current proposal, the method is applied to the X-array and 50% of the science signal is devoted to calibration, which means that the method only has an effect for OPD perturbations beyond 10 μm. Further research is required to investigate if a smaller fraction of the science signal can be used for low-frequency calibration, and whether the method is also suitable for the TTN.

Whether these post-processing methods are actually required is the topic of an ESA contract for an end-to-end simulator in which the noise perturbations, control loops and data processing are modelled in a realistic manner.

4. DARWIN TECHNOLOGY STATUS

4.1 Core technology

In this section some of the core technologies currently underway which are necessary to be demonstrated to ensure the success of the Darwin mission are described.

4.1.1 Wavefront Filters

Wavefront filtering in the infrared waveband is an enabling technology for Darwin. It is known that wavefront errors as small as a few nanometres rms will degrade the Darwin nulling performance. In theory, wavefront errors could be simply removed by propagating the recombined beam through a short length of single-mode waveguide, thanks to the waveguide's modal filtering properties. Technically, waveguides can be realised in either single mode optical fibres or integrated optics.

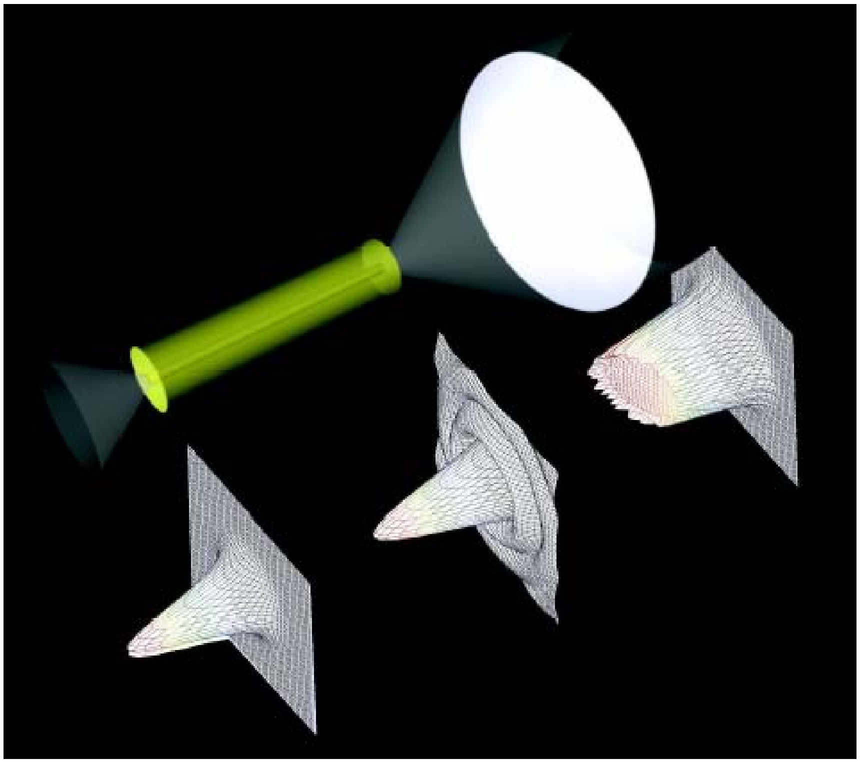

Figure 4.1.1: Concept of modal filtering by single-mode fibres.

4.1.2 Single-Mode Fibres

Two parallel activities, led by EADS Astrium GmbH (D) and TPD/TNO (NL), were successfully concluded end of 2004 and early 2005 respectively, delivering and testing first samples of single-mode step-index fibres for Darwin.

Specifically the EADS Astrium team manufactured 35 fibre samples using different materials and processing techniques. GaAsSeTe (GAST) chalcogenide fibres were produced, suitable for operation in the 5-10 micron range, featuring high quality in terms of core shape and material homogeneity. Single-mode operation has been demonstrated at 10.6 micron, with typical losses (including Fresnel losses) of 73.5 dB/m (with V=0.76 at 10.6 micron). The team also developed fibres made of poly-crystalline silver halide (AgBrCl) for operation at wavelengths up to 20 micron. The crystalline structure of AgBrCl makes fibre manufacturing considerably more difficult than for chalcogenide glasses. The samples exhibit larger core defects and irregularities than the glassy ones. However, single-mode behaviour at 10.6 micron has been demonstrated, with attenuation (including Fresnel losses) of 23.2 dB/m (V=1.34 at 10.6 microns). The quality of AgBrCl fibres can be improved by systematic optimization of material purity and the manufacturing process.

The team led by TPD/TNO developed TeAsSe (TAS) chalcogenide fibres, with an operational range of 4 to 12 micron. Single-mode fibres of very good quality have been obtained, with typical attenuation of 10-18 dB/m. Both activities have shown the need to have high absorption coatings applied on the cladding external surface, in order to damp leaky modes that tend to propagate through the fibre because of the finite cladding diameter dimension. Suitable absorbing materials have been identified for both chalcogenide and silver halide fibres, and their effectiveness has been demonstrated experimentally. In addition both activities have demonstrated that contrary to theoretical predictions which state that only a length of a few mm is required to damp the leaky modes assuming infinite cladding diameter, the fibres need to be longer than 20 cm to damp all leaky modes and behave as a single mode fibre.

A new generation of tellurium glasses has recently been discovered, characterised by good transmission in the far infrared region, up to 25 µm. The study “Development of Te-Glass” has recently been initiated under an ESA contract to conduct glass engineering work and perform characterisation on Te-glass as a candidate material for optical fibre manufacturing satisfying the DARWIN requirements. The quaternary glass type TGGI and, alternatively, the ternary glass type TGI are considered as strong candidates for DARWIN waveguides. The second objective of this activity is to perform preliminary fibre manufacturing in order to determine the suitability of the Te-glass for fibre production. Preliminary testing of the produced fibres is performed with the guiding properties and transmission losses being determined. Preliminary attenuation measurements show an almost flat coefficient between 3 and 20 microns. Drawing of purified mono-index fibres was successful revealing a minimum attenuation of 0.45 dB/cm at around 12 microns, with an improvement of the transmission at liquid nitrogen temperatures by a factor of

2. Further results in the course of this activity will allow the Agency to establish whether Te-glass is a viable option for the Darwin single mode waveguide.

Based on this work a follow-on activity “Single Mode Waveguide” will focus on the development of reliable manufacturing techniques that can produce single mode waveguides based on step index fibres. The activity should establish the reproducibility of the manufacturing process of wavefront filters that are good enough to achieve the required nulling performance of DARWIN.

4.1.3 Integrated Optics

At telecom wavelengths, a number of optical functions relevant to interferometry have already been realized and demonstrated using integrated optics (IO) technology. The activity “Photonic Devices for Multi-Aperture Imaging Interferometer” was performed under ESA contract and demonstrated the feasibility of an IO chip performing the functions required in a 3-telescope interferometer. For the first time, an all-waveguide 3-telescope interferometer with science recombination and metrology has been designed, built and validated at system level.

For operation in the 4-20 micron spectral range, a team led by IMEP (F) has been investigating IO approaches including identifying materials, and developing manufacturing technologies for single-mode IO components. Cryogenic operation at 40K was not a requirement in this activity. Both conventional dielectric waveguides and metallic hollow waveguides concepts have been addressed, together with possible manufacturing technologies. Metallic hollow waveguides (MHW) and thin-film dielectric waveguides were selected for actual realization and testing. Elementary linear and curved waveguides, T-junctions and a two-beam combiner have been characterized. The MHW samples have proven to be extremely effective as modal filters allowing for nulling ratios between 10^3 and 10^4, although they operate in single polarization only. Metallic hollow waveguides would be capable of operating in the 4-18 micron wavelength range but suffer from high coupling and intrinsic propagation losses that prevent their use for more complex functions. The waveguides produced during this ESA study showed a typical transmission of only 1% over a length of 1 mm. Dielectric waveguides based on Tellurium glasses have a better potential in this respect. The critical issues for dielectric waveguides are the composition of a pair of glasses suitable for the design of a waveguide and their purification in order to minimize absorption bands.

Given the potential of reducing DARWIN bulk optics to the size of a chip, offering great simplifications of thermal control and mechanical stability, a follow-on activity “Integrated Optics Components” will in particular establish reliable and reproducible manufacturing techniques based on dielectric waveguides. Demonstrator components will be built and their performance validated.

4.1.4. Waveguide Coupling

4.1.4.1. Step index fibres

The maximum achievable coupling efficiency for a non-obscured uniformly illuminated circular aperture is less than 80%, due to the mismatch between the Airy disk profile of the focused incoming beam and the approximated Gaussian profile of the fundamental mode of the single mode fibre. Work through two parallel contracts is underway by two teams led by Contraves (CH) and KDA/Sintef (N), respectively, to identify and breadboard advanced concepts for coupling optical radiation into single mode waveguides that minimize the total insertion loss. Both teams are currently carrying out the detailed design of a proof-of-concept demonstrator operating at near infrared wavelengths. Presently, analyses show that a coupling efficiency larger than the theoretical maximum of about 80% is possible taking into account implementation losses (e.g. optical losses due to the additional optical elements, manufacturing tolerances and alignment errors).

4.1.4.2. Holey Fibres

The problem of high chromatic coupling losses of light into the waveguide and limited bandwidth due to the excitation of higher order guided modes has been addressed in a study of photonic crystal fibres for space applications. Holey Fibres (or: index guiding photonic crystal fibres) are based on two-dimensional structures with a refractive index variation in the plane perpendicular to the fibre axis and an invariant refractive index structure along it. The cladding of the fibre is formed, in general, by a periodic structure of air holes at wavelength scales, embedded in some dielectric material. The guiding in this fibre type results from the average index of the holey cladding, which is lower than of the solid core and light is confined to the core via the same mechanism that is responsible for guidance in a step index fibre. Computer modelling has indicated the high potential of avoiding chromatic coupling losses by using this fibre type.

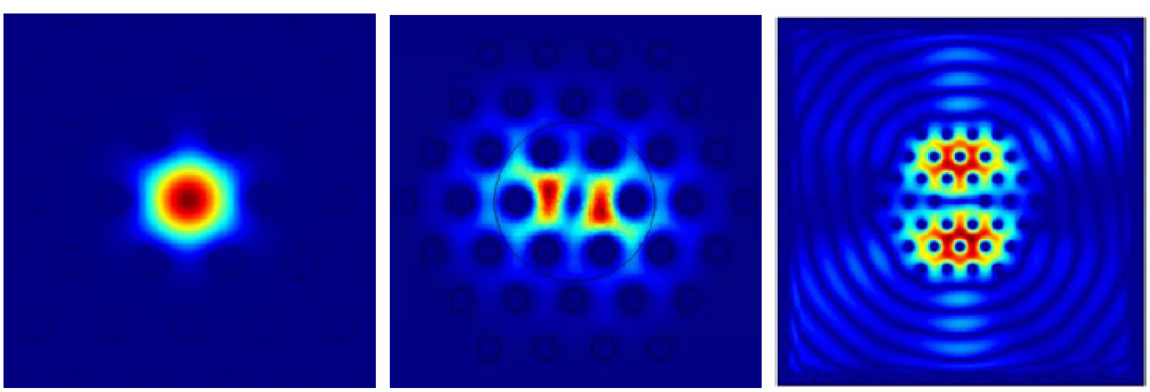

(a) (b) (c)

Figure 4.1.2: Examples of (a) a fundamental modal field, (b) a moderately leaky higher-order mode and (c) a highly leaky higher-order mode of a photonic crystal fibre. (Simulation produced under ESA contract by Hovemere Ltd.)

4.1.5 Achromatic Phase Shifter

The main requirement on the APS is that it shall have the potential to provide a rejection rate of 1E-6 or better in the 6-18 μm spectral range (goal: 4-20 μm), with a transmission of better than 95%. Three APS systems have been selected for breadboarding. Two reflective concepts exploit the reversal of the electric field at reflection or at focus crossing, respectively. These methods can only produce π phase shifts, as required,for example, by the X-array. The third APS concept makes use of a stack of three dispersive wedge plates (Ge, ZnSe and KRS-5) to compensate the dispersion characteristics, as done with achromats. Non-π phase shifts can be produced with this device. Note that for example, TTN requires 120° phase shifts. All three APS devices have been built and characterized. The reflective APS devices will be tested in a nulling configuration at short wavelengths (2-3 micron). A dedicated 100 K nulling testbench is being prepared for the final validation of all APS devices under cryogenic conditions and broadband illumination at 6-20 micron.

A separate technology development study has been recently initiated addressing a different APS concept, based on total internal reflection zeroth order grating. Zeroth Order Gratings (ZOG) consist of sub-wavelength structures for which only zeroth-order transmitted and reflected light is allowed to propagate. The use of ZOG structures as antireflection layers for the Darwin refractive optics (beam splitters, cross combiners, wedge APS) is also being investigated.

4.1.6 Infrared Detector Arrays

Impurity band conductors (IBC) – e.g. Si:As – are regarded as the present baseline detector for the Darwin mission, in view of their high Quantum Efficiency (> 50% over the entire spectral range), low read noise (less than 10 e^-) and low Dark Current (< 25 e^- sec^{-1} pix^{-1}). However, they require cooling to a few (~6-8) K which leads to heavy system costs and a mass penalty, and to mechanical vibrations that are difficult to isolate from the optical bench. Currently an ESA study is investigating the potential to raise the operational temperature of IBC detectors. The design of the demonstrator, including different geometrical pixel configurations, is almost complete and requires further processing optimisation of the buried contact to avoid severe dopant diffusion into the active pixel area. In addition, the readout circuit design is shared with the QWIP activity (see below).

The decision concerning the cooling philosophy for Darwin is of utmost importance: on the one hand vibrations must be avoided thus a purely passive cooling is being sought, on the other hand, the very critical detector performance must be assured. A development activity is

ESTEC
Keplerlaan 1 - NL 2201 AZ Noordwijk ZH - The Netherlands
Tel (31) - Fax (31) -

underway with the goal to establish and demonstrate the performance of a detector meeting the Darwin requirements at the highest possible temperature. The selected technology is Quantum Well Infrared Photodiodes (QWIP). Initial theoretical modelling gave hope that the Darwin dark current requirements could be met around 16 K. Two array demonstrators have been manufactured, optimized for the shortest and longest Darwin wavelengths. Tests on the finished samples were done last year. Dark current measurements did not meet the requirements, but the reasons for the discrepancy from theory are understood. It is expected that further developments may reduce dark current to the right order of magnitude. However, the quantum efficiency of these devices is low, even after the implementation of a dedicated on-pixel grating to allow polarization-independent absorption. This has essentially ruled out these sensors for Darwin. Dark current optimization is currently being pursued since QWIP technology is likely to find broad applications in both science and Earth observation missions.

4.2 Subsystems development

4.2.1 Optical Delay Line

The Optical Delay Lines (ODLs) have the task to stabilize and equalize the optical path lengths between the DARWIN science beams, without introducing any optical asymmetry that might degrade the nulling performance. Main critical requirements include a path length stability of better than 1 nm RMS at a control bandwidth of 10 Hz, over an optical path length range of at least +/-10 mm. Since the ODL is the actuator of the Fringe Tracking control loop, it is assumed that the appropriate metrology signal is made available to the control electronics commanding the delay lines in order to achieve the performance. Two activities are underway aimed at designing, manufacturing and testing delay line units compatible with the DARWIN optical requirements, at vacuum and 40 K temperature operating conditions. The ODLs will be representative in form/fit/function of an engineering model.

One development concept involves a cat-eye optical element which is guided by an active magnetic suspension system. Another design is based on a corner cube optical element, guided by a passive flexure mechanism suspended in an isolation stage. In both cases, the ODL moving mass is less than 0.7 kg, and coarse actuation is provided by a single-stage voice coil device, simplifying the control electronics compared to a typical dual-stage delay line configuration. Both approaches have been successfully tested with respect to the critical subsystems at cryogenic temperatures (optical elements, actuator, and guiding mechanism). Further activities involve conducting development test activities for the complete optical delay line system at ambient and at low temperature.

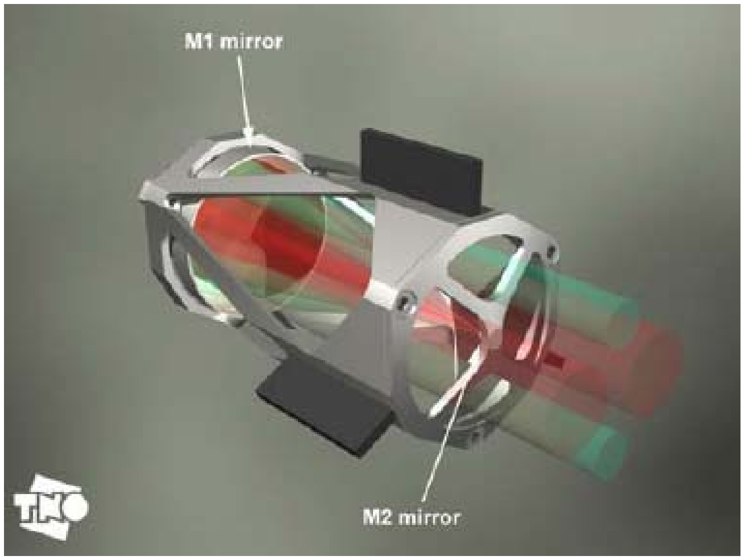

Figure 4.2.1: A compact breadboard cryogenic delay line representative of a flight mechanism has been built under ESA contract. (TNO, in cooperation with Micromega-Dynamics, SRON, Dutch Space and CSL).

4.2.2 Fringe Sensor

In order to maintain a deep null despite environmental disturbances (relative displacements of the flyers, vibrations, thermal effects), optical path differences must be measured at sub-nanometric accuracy, with a frame rate of at least 10 Hz. An activity is underway for the development of a DarWin AstRonomical Fringe sensor (DWARF) for this purpose. The selected DWARF concept operates at visible wavelengths, with the provision for an additional, near-IR channel for redundancy. Beams are coherently combined in the image plane. OPD, tip-tilt, defocus, and higher-order aberrations are simultaneously estimated from the resulting fringe pattern, using phase diversity techniques. Wavefront sensing capabilities are required to calibrate phase errors arising from the process of coupling aberrated beams into a fiber. This effect cannot be measured directly by the fringe tracker. A three-beams test setup has been built including an optical system with which controlled amounts of aberrations can be introduced in one beam. Performance tests have demonstrated the validity of the all-in-one focal plane approach to accurately measure aberrations of the multiple-aperture instrument. The DWARF breadboard has proved to be compliant with the requirements, except for real-time defocus measurement at 10 Hz for which real-time algorithms need further development.

4.3 Technology breadboards

In the years 2001-2003 two parallel studies "Multi-Aperture Imaging Interferometer" were carried out to design, manufacture and test a breadboard of an optical two-arm interferometer and to demonstrate the feasibility of deep nulling of a point source and of imaging of an extended source. Such demonstrations were in a first step successfully made at NIR wavelengths (1550 nm) down to suppression ratios of 1E-5 for unpolarised light, allowing for operation in normal laboratory environment.

4.4 Software simulators

4.4.1 DARWINsim

DARWINsim is a high-level routine to assess the science output of the NIRI / Darwin mission in terms of number of target stars that can be screened for the presence of planets, and subsequently be followed up with spectroscopy, as a function of configuration parameters, mission duration and astronomical conditions and based on a specified target catalogue. Although its current status is mature, some development is ongoing as technological knowledge advances. The power of DARWINsim, is its relative simplicity which allows to obtain statistics for a target catalogue, is also it's main weakness. Detailed computation involving time-resolved assessment of control loops, GNC or polarization issues are not possible.
In near term it will provide a cross-check of science performance figures from the System Assessment Studies. On the longer term, the code may eventually develop into the Mission Planning Tool for the definition of the NIRI / Darwin mission observation plan and strategy.

4.4.3 FINCH / OPT

It can be assumed that each of the Darwin subsystems will be tested before launch, but given the complexity of the Darwin system it seems unlikely that a realistic integrated test of the full system is feasible. With detailed knowledge of the subsystems and their performance, it is however possible to perform full system simulations. The FINCH software suite is being developed to this end and is coded in MatLab and SimuLink, and is supported by BeamWarrior ray-tracing software.

As a first-principles ray-tracing tool BeamWarrior is capable of tackling most optical problems that may arise during the Darwin optics development. BeamWarrior output is used to generate Sensitivity Matrices which are then used by FINCH / OPT to allow a time-resolved simulation of an observation, eventually including array rotation, detector operation, control-loop functionality.

Straylight issues, however, can not be addressed with this code. The raison d'etre for FINCH / OPT, is at the same time its main weakness. The set-up of realistic simulations requires a fully developed optical design, in which all the optical elements are specified in terms of positions, alignments and optical characteristics.

FINCH has the potential to become an extremely detailed, accurate end-to-end simulator for Darwin, with the capability to address simultaneously complicated optical issues, and will probably be the only tool to provide an integrated view on the performance of all the Darwin subsystems in L2.

4.4.4 ICC / GNC (a.k.a. FINCH / GNC)

ICC is a software tool for the simulation of Guidance and Navigation Control of a Formation Flying array of telescopes. In view of the instability noise problem, it will be necessary to update the code so that it generates the micro-vibration frequency spectra that form part of the perturbation background, and that are induced by internal and external influences (coolers, FEEPs). These results would be used to drive a Finite Element Model of the spacecraft to assess the micro-vibration environment of the optical path.

4.4.5 RESSP / ORIGIN

This is software for the generation of detailed source scenery, including the planetary system, stellar disk, local and exo-zodiacal flux, galactic emission, background stars and galaxies, in the form of a stacked set of three or four-dimensional maps (x, y, λ, t) in FITS format. It provides the input for FINCH / OPT or RESSP / PINSON.

4.4.6 RESSP / FITTEST

This is software for the reconstruction of the planetary positions and spectra from the Darwin science and housekeeping data, expected to form the core of the Darwin data reduction pipeline. Fittest will be used for a comparative performance assessment of the NIRI TTN and X-array configuration designs. A further development is required to take into account the instability noise problem.

4.4.7 RESSP / PINSON

The PINSON software will have the extra advantages of being coded in a more portable language and to allow interfacing with ORIGIN and FITTEST for end-to-end testing of the basic data-reduction pipeline. In a later stage, an interface with the ICC / GNC software will be added to allow implementation of instability noise. In the greater scheme it also bridges the gap between

DARWINsim (too high level) and FINCH / OPT (not yet developed to sufficient functionality and too complex for a lot of tests).

4.4.8 Simulators Overview

The starting point is the target catalogue, with currently 608 candidate targets. A top-level code like DARWINsim is used to obtain an idea of what science can be expected. It also provides for each candidate an optimised baseline, and the wavelength range which is most suited for water spectroscopy.

For an individual case, e.g. selected on the basis of DARWINsim output, a source scenery can be generated with ORIGIN. In order to have a realistic time-resolved simulation the ICC / GNC provides input perturbations for the OPD and tip/tilt, resulting from residual differential spacecraft drift, residual S/C attitude fluctuations and thruster noise, remaining after the Guidance and Navigation Control loops. In principle a Finite Element Modeling (FEM) code, fed with the GNC thruster impulses, should be used to assess the OPD and tip/tilt perturbations due to micro-vibrations, or to establish that the S/C transfer function does not transmit such noise to a harmful level. Having a fully specified scenery, plus a fully specified optical model, both as a function of time, it is in principle possible to simulate the full set of science and house-keeping data. This set of data is then used by FITTEST to reconstruct the positions and spectra of the planets. Comparison with the original scene then allows to either update the technical requirements, or to improve the mission science predictions.

Finally PINSON is a short-cut that by-passes the complicated set-up of a FINCH simulation, to allow a focus on a specific problem, either testing of the FITTEST algorithm, or the impact of instability noise on planet detection and spectroscopy with a simplified physical description. Eventually, FINCH will be applied to perform a comprehensive assessment of the fully integrated DARWIN system, and to discover problems hidden in the system complexity.

4.6 Formation flying:

4.6.1 Guidance, Navigation, and Control

The development of guidance, navigation and control (GNC) algorithms for precision formation flying has been addressed in the TRP (Technology Research Program) studies “Interferometer Constellation Deployment” and “Interferometer Constellation Control”.

The first activity has covered the deployment modes of the Darwin interferometer, namely the jettisoning from the launch dispenser, the transfer from Earth to the L2 orbit and the creation of the baseline control mode of the formation. In the deployment phase, the GNC system makes use of the *milli*-Newton propulsion actuators. The sensors it uses are the RF system for relative distance measurements between spacecrafts, gyros for spacecraft despin, star trackers and coarse sun sensors. The GNC design controls all relative positions and attitudes between the spacecrafts. A GNC design tool as well as a simulator have been developed including a Monte Carlo capacity for the statistical properties.

The study “Interferometer *Constellation* Control” has developed the GNC algorithms for formation flying during the operational phase. The activity dealt with the design of the 3 fundamental modes of the Darwin interferometer, namely the Baseline Control Mode, the Fringe Acquisition Mode and the Nominal Mode. The sensors involved are the RF system for the coarse modes, and the High Precision Optical Metrology systems for the other modes. The GNC system makes use of two actuation systems: the *micro*-Newton propulsion system and the Optical Delay Line actuator.

The GNC must control all relative positions and attitudes between spacecraft, as well as the delay line stroke for equalizing the optical paths of the beams at combination to within the coherence length. A GNC design tool as well as a simulator have been developed including a Monte Carlo capability for statistical analysis.

4.6.2 Metrology

A number of metrology systems will measure attitudes and relative positions of the telescopes, as needed by the control system to deploy and control the formation. A chain of metrology systems allows the measurement accuracy to be refined both in terms of spacecraft pointing and relative positions. A number of coarse sensors, including coarse sun sensors, star trackers and Radio Frequency metrology, are utilized in the initial stages ensuring that the attitudes and positions are good enough to hand over to the subsequent laser metrology systems. Laser metrology systems will bring the relative attitudes and positions to a sufficiently accurate level to start the Fringe Acquisition Mode. In this mode the differential optical path lengths are controlled to nanometer accuracy and the Optical Delay Lines are actuated such that stellar fringes can be detected on the Fringe Sensor.

Figure 4.6.1: Photograph of a Radio Frequency Receiver/Transmitter built under ESA contract.

4.6.2.1 Radio Frequency Metrology Subsystem

The Radio Frequency (RF) Formation Flying metrology subsystem is the first element in the metrology system chain (together with sun sensor and star tracker). These sensors will ensure initial good attitude and position accuracy for the subsequent metrology systems. The RF metrology provides autonomous restitution of coarse position and attitude throughout all mission phases.

The development of the RF metrology has been addressed in the TRP study "Formation Flying RF Subsystem" is proceeding in the study "RF Metrology Subsystem".

The first activity focused on the design of the Darwin RF metrology, the development of a breadboard to demonstrate the main features of the concept and the investigation of performances based on laboratory experimentation.

Following a decision by the ITU to protect the GPS L-band frequencies it is no longer possible to use S-band equipment as developed in the first study. Furthermore, following detailed analyses it has become evident that a dual carrier frequency is required in order to reach the required performance of the RF metrology subsystem. In order to overcome the limitations of the breadboard developed in the first study, a second study "RF Metrology Subsystem" was initiated to develop an engineering model. This engineering model shall be designed, breadboarded and tested and shall be representative of the software and hardware functionality and the electrical design of the final flight unit. It shall be realised on a single board, minimizing size and mass. The elegant breadboard shall consist of two and three nodes, allowing end-to-end performance demonstration.

4.6.2.2 Optical Metrology

Once the coarse sensors have ensured that the attitudes and positions of the spacecrafts are good enough, subsequently a laser metrology system will bring the relative attitudes and positions to the sufficiently accurate level for fringe acquisition. The development of "High Precision Optical Metrology" has been addressed in an ESA study in which a fine lateral sensor and two longitudinal sensors were breadboarded.

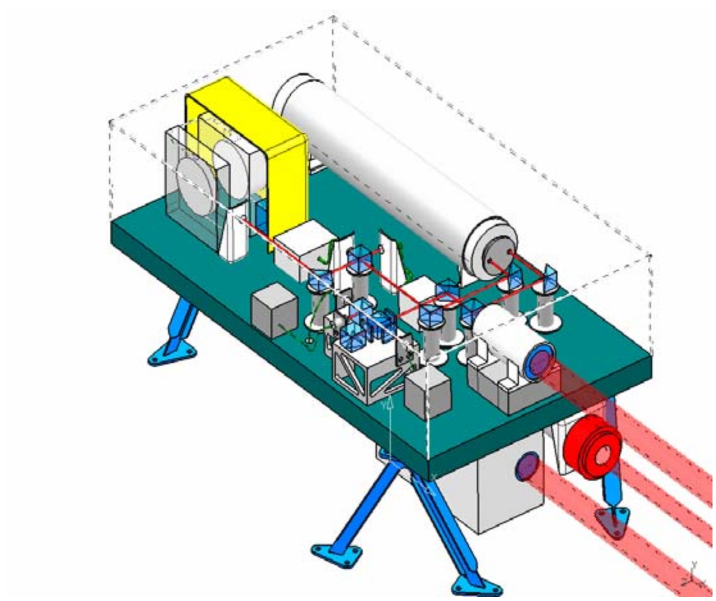

Figure 4.6.2: Design of an optical metrology breadboard built under ESA contract.

In case the out of plane performance of the radio frequency metrology system turns out to be not good enough for the fine lateral sensor, a *coarse* lateral sensor (CLS) can be used, which would be based on a *divergent* beam whose back-reflected light (from a corner-cube) is imaged onto a CCD camera. The coarse lateral metrology can thus provide absolute measurements of the position of a spacecraft in the plane perpendicular to the beacon from the reference satellite, with an accuracy of 1 mm @ 10 Hz.

The *fine* lateral metrology monitors absolute displacements of a spacecraft in the plane perpendicular to the beacon from the reference satellite, to an accuracy of 32 µm rms @ 10 Hz, within the range of the coarse lateral metrology (±1 mm). The fine lateral sensor transmits a collimated beam (25 mm) from one spacecraft to another, where a large area detector measures the lateral offset. The lateral offset is determined by fitting a Gauss function over the received irradiance to calculate the centre of gravity of the received light. This measurement, together with the fine longitudinal metrology, allows to damp OPD drifts to a level compatible with fringe acquisition.

The longitudinal absolute laser metrology system monitors the distance between two spacecrafts to an accuracy of 32 µm rms @ 10 Hz. The bulk of this metrology system (two frequency-locked Nd-Yag lasers, send/receive optics, electronics) is hosted on the beam combiner satellite. The metrology beam is sent to the collector spacecraft, where it is retro-reflected. In order to determine the longitudinal distance, an interferometer is fed from the two frequency-locked lasers. The phase-difference of the interference fringes from the two laser frequencies determines the distance. Such a dual-wavelength interferometer acts like a single wavelength interferometer with a new synthetic wavelength, which is given by the product of the two laser frequencies divided by their difference. The synthetic wavelength is chosen such that the interferometer's ambiguity range covers the inaccuracy range of the radio frequency metrology. The metrology path is independent from the science one, which greatly simplifies beam routing. Analysis has shown that the non-common paths between the science and metrology beams can be kept well within the required measurement accuracy.

4.6.3 Propulsion

Spacecraft propulsion is required for two functions:

1) Orbit correction, in order to correct for launcher dispersion, and possibly for injection in small-amplitude orbit at L2. This could be achieved with a chemical propulsion system, or with milli-Newton thrusters.
2) Formation flying (FF), including both
   a) coarse manoeuvres, e.g. slew, and
   b) precision formation control

For FF coarse formation manoeuvres, a thrust capability of a few milli-Newton and a resolution of ~ 0.1 mN would be required. Precision formation flying will make use of µN thrusters with a maximum thrust of ~ 0.1 mN and µN-level resolution, which will allow performing fine attitude/position corrections directly during an observation, without perturbing fringe tracking. Possible technologies for mN and µN propulsion have been examined and traded-off during a recent ESA internal trade-off.

For the DARWIN coarse manoeuvres, which include reconfiguration and rotations, Cold Gas Microthrusters (CGMT) and Electric Propulsion System were found to be the most suitable propulsion technologies. Because CGMT thrusters require a considerable amount of fuel due to their low specific impulse, the Electric Propulsion System technology is today considered the baseline for this application. Several electric propulsion systems exist nowadays and have already been operated in space, e.g.,

- "RIT-10" developed by EADS Space Transportation, Flight Proven in ARTEMIS
- "T5" developed by QinetiQ, Flight Proven in ARTEMIS
- "Radio-frequency with Magnetic-field ion Thruster" developed by Alenia Spazio, Laben Proel, Engineering Model
- "Mini-HET" developed by ALTA, Engineering Model

For the DARWIN micro-Newton manoeuvres, such as fine pointing and slow OPD control during science operation, two different technologies, Cold Gas Microthrusters (CGMT) and Electric Propulsion Systems were taken into consideration as propulsion system. CGMT option is currently not suitable due to mass constraints. The following options are currently under investigation:

- "FEEP-8"
- "Indium FEEP Multi-emitter"
- "RIT-4 micro-Newton ion thruster"
- "Radio-frequency with Magnetic-field ion Thruster"

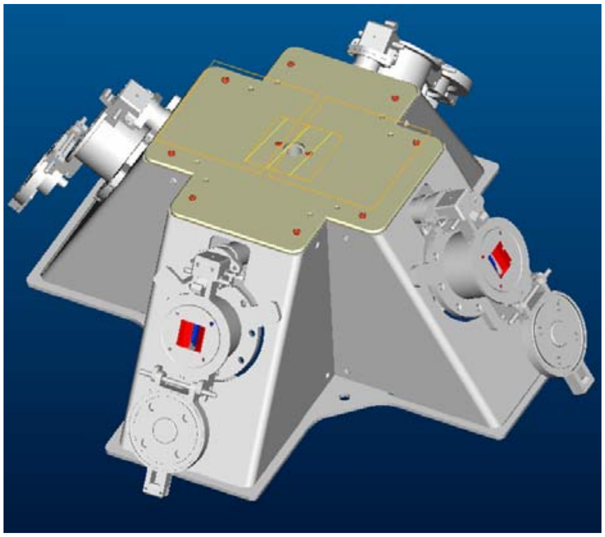

Figure 4.6.3: Design of a micropropulsion engine built under ESA contract.

4.6.4 Formation flying demonstration

Generally it is considered to perform testing and validation of all formation flying components, sub-systems and systems as far as possible on their own level (e.g., by traditional representative pseudo-static test beds). The main areas of sub-system validation would be metrology, actuation and control. The final formation flight validation is expected to occur in one or more, potentially modular, FF test facilities, depending on their added value, e.g., given by system-level component interplay or where subsystems are affected by the satellite environment. In an endeavour to isolate the technical implementation issues of formation flying from overall programmatic issues of the Cosmic Vision themes and mission choices, a "Definition Study for a Formation Flying Ground Testbed" has recently been initiated. Its major goals are to capture the formation flying requirements of XEUS and Darwin, and to propose test methodologies to provide validation, together with a baseline design proposal. The route currently embarked upon is to follow a phased approach that does not a priori prescribe a demonstration flight or purely ground test bed approach to FF validation.

4.6.4.1 Ground Testbeds

Testing has to be done on ground as far as at all possible as the required investment for space testing is in general far greater than that of even very elaborate and extensive ground testing facilities. Moreover, the flexibility of ground facilities is far superior to space demonstrations and allows the testing of an extensive parameter and scenario space, and the testing of a vast range of hardware and software options and permit the use of state-of-the-art complex test systems. After having captured the FF requirements by the above mentioned definition study, a detailed design activity may follow.

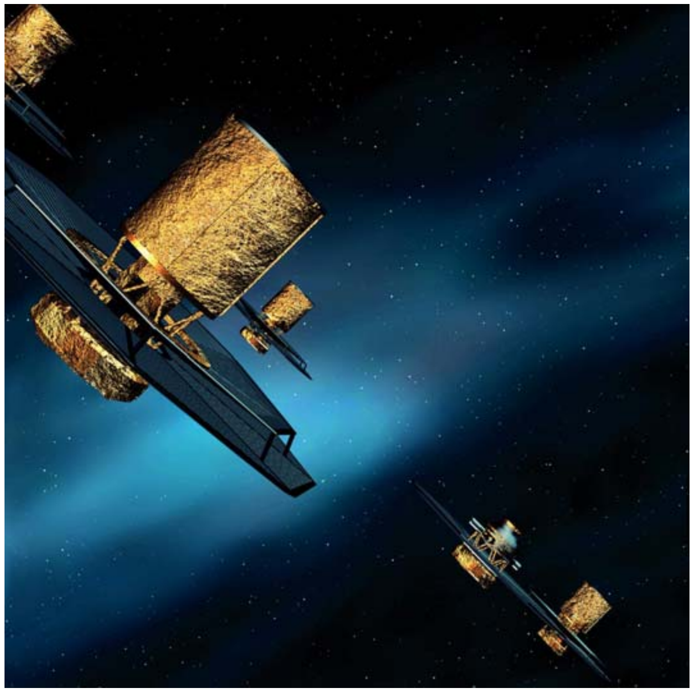

Figure 4.6.4: Artist's impression on DARWIN spacecrafts flying in formation.

5 SUMMARY

Studies on the nulling infrared interferometer mission for detection and characterization of extra-solar planets continue as planned as this is a dominant theme within the new Cosmic Vision Programme. The system assessment study activities have been completed, with final presentations held in Estec in October 2006. These two parallel system studies have focused on establishing possible optical architectures and the associated system level solutions and expected science performance. These preliminary studies have allowed increasing the definition of the mission architecture, to identify specific critical areas and to establish the trade-off between science performance, technical complexity and risk.

There are two different interferometer configurations. One is an innovative interferometer configuration, the so called out-of-plane TTN array, comprising three telescope collecting spacecrafts and one beam combiner spacecraft. This solution, which given its novelty has less study heritage, proved promising given a number of simplifications in the S/C design, although the optical architecture of the beam combiner spacecraft would be more complex and is calling for additional definition work. The TTN solution is compatible with the constraints posed by a dedicated Ariane 5 ECA launch to L2, providing some development in the manufacturing of large lightweight space astronomical mirrors. The simplified system configuration (fewer deployments, more compact S/C design), combined with one less spacecraft, have the potential for reduced development and operation risk.

The second configuration investigated is the so called X-array comprising four telescope collecting spacecraft and one beam combiner spacecraft. This configuration, benefiting from a longer study heritage and also investigated by the TPF-I team in the US, has a simpler beam combination scheme on the beam combiner spacecraft. However, the telescope collector spacecrafts have additional complexity through the deployment requirements of M2 mirrors, large area sunshields and even service module. The presence of a fourth collecting telescope poses problems in accommodating the spacecrafts in the launcher, both in terms of total mass and volume. On this basis, the investigated X-array configuration is compatible with the Ariane 5 ECA capability only under the assumption of complex deployment schemes and reduced primary mirror diameters. The mass constraint nevertheless requires some development effort in the manufacturing of lightweight space astronomical mirrors.

The compared performance of the X-array planar and TTN non-planar configuration were estimated assuming that two mission concepts shall be launched with an Ariane V ECA into L2. The direct consequence of the launcher selection is that larger collecting mirrors can be implemented in the TTN non-planar concept. The X-array planar configuration has however inherent advantages. It provides a higher spatial resolution useful to disentangle multiple planet signals. The post-processing of the X-array data allows a partial removal of the instability noise by using a stretched imaging baseline. This has the potential for relaxed requirements on OPD and intensity control accuracy that are difficult to achieve. The symmetry of the X-array optical scheme is kept during rotation which prevents any residual

ESTEC
Keplerlaan 1 - NL 2201 AZ Noordwijk ZH - The Netherlands
Tel (31) - Fax (31) -

signal modulation due to polarization. Nevertheless, for an Ariane V launch in L2, the orthogonal-TTN non-planar architecture is an attractive alternative since it has the potential for similar science performance with only three collector spacecrafts. This can be explained by the fact that (i) the better sky access of the non-planar TTN (and therefore the access to easier targets), (ii) the larger telescope diameters of the TTN that can be accommodated in an Ariane V launcher, and (iii) the smaller sunshields of the TTN (that enable smaller baseline specially for nearby stars) compensate the intrinsic performance advantages of the X-array concept. Ongoing mission analysis has shown that the optimum profile, with respect to transfer logistics and costs, is presently seen to be through all spacecraft being accommodated on a single launcher and launched to L2. The performance of the mission would clearly benefit from an increase of the launching mass and volume capability of the launcher.

Planned future activities

The results of the system assessment study have demonstrated the need to develop a detailed end-to-end simulation tool, capable of establishing the science performance of different interferometer configurations and the related drivers including such issues as optical path differences stability, intensity control accuracy, polarization matching, …etc. This is a complex issue involving a proper description of the target source properties, optical architecture, perturbation effects by differential solar pressures, sensors and actuator noise, spacecraft thermo-mechanical architecture, guidance navigation and control of the constellation at L2 and data processing techniques. It is therefore planned during 2007 to improve the Darwin simulation tools, in view of providing simulation capabilities enabling to establish the performance capability of the identified mission concepts.

As described previously, candidate architectures for the Darwin mission have been established during the parallel system assessment studies conducted in 2006. Two candidate space segment concepts were defined as a satellite formation. One concept consists of three telescope spacecrafts and one out-of plane beam combiner spacecraft and is referred as the orthogonal out-of plane TTN or EMMA concept. The other mission concept consists of a four telescope spacecrafts and one in-plane beam combiner spacecraft and is referred as the in-plane X-array concept. It has been decided to increase the definition level of these concepts by (i) consolidating their beam combiner payload design and (ii) specifying the technology development activities (with corresponding functional and performance objectives) that would be required to demonstrate on-ground the feasibility of the Darwin mission. This will be implemented through a CCN to each of the two existing parallel contracts.

Concerning ESA internal work, it is envisaged to prepare a test-bed implementation plan The prime technology driver would be to demonstrate the required nulling (10-6) in the relevant wavelength region 6-20 µm at cryogenic temperatures on a nulling breadboard. This representative nulling breadboard is viewed as the key development necessary to ensure the mission's technical feasibility. The TDP will be revised based on the final conclusions of the current system level studies.

6 REFERENCES

6.1 References related to Darwin technology

[1] Haaksman, Ron P. H., et al.: "A combined nulling and imaging pupil-plane beam-combiner for DARWIN" SPIE 6268 (2006),

[2] van den Dool, T. C., et al.: "The DARWIN breadboard optical delay line verification programme" SPIE 6268 (2006),

[3] Ergenzinger, K., et al.: "System driven design and validation of a cryogenic optical delay line for DARWIN" SPIE 6268 (2006),

[4] Cheng, Lun K., et al.: "Development of broadband infrared single-mode fibers for the DARWIN mission" SPIE 6268 (2006),

[5] Mocoeur, Isabelle, et al.: "DARWIN fringe sensor: experimental results on the BRISE bench" SPIE 6268 (2006),

[6] den Hartog, R.; Absil, O.; Gondoin, P.; Stankov, A.; Augerau, J. C.; Du Forresto, V. Coudé; Mourard, D.; Fridlund, M.; Gitton, P.; Puech, F.; and 3 coauthors 2006, Direct Imaging of Exoplanets: Science &Techniques. Proceedings of the IAU Colloquium #200, Edited by C. Aime and F. Vakili. Cambridge, UK: Cambridge University Press, 2006., pp.233-239, " The prospect of detecting exo-planets with the Ground-based European Nulling Interferometer Experiment".

[7] Wallner, Oswald, et al.: "DARWIN mission and configuration trade-off" SPIE 6268 (2006),

[8] Coudé du Foresto, V., et al.: "ALADDIN: an optimized nulling ground-based demonstrator for DARWIN" SPIE 6268 (2006),

[9] Absil, O.; den Hartog, R.; Gondoin, P.; Fabry, P.; Wilhelm, R.; Gitton, P.; Puech, F. 2006, Astronomy & Astrophysics 448, 787 ``Performance study of ground-based infrared Bracewell interferometers. Application to the detection of exozodiacal dust disks with GENIE"

[10] Fridlund, C. V. M., et al.: "Status and recent progress of the Darwin mission in the Cosmic Vision program" SPIE 6268 (2006),

[11] Karlsson, A., et al.: "Darwin: a mission overview" SPIE 6265 (2006),

[12] Martijn, Henk, et al.: "Far-IR linear detector array for DARWIN" InPhT 47 (2005), 106

[13] Cheng, Lun K., et al.: "Test results of the infrared single-mode fiber for the DARWIN mission" SPIE 5905 (2005), 447

[14] P. Gondoin, R. den Hartog, M. Fridlund, P. Fabry, A. Stankov, A. Peacock, S. Volonte, F. Puech, F. Delplancke, P. Gitton, A. Glindemann, F. Paresce, A. Richichi, M. Barillot, O. Absil, F. Cassaing, V. Coude du Foresto, P. Kervella, G. Perrin, C. Ruilier, R. Flatscher, H. Bokhove, K. Ergenzinger, A. Quirrenbach, O. Wallner, J. Alves, T. Herbst, D. Mourard, R. Neuhauser, D. Segransan, R. Waters, G.J. White 2005, proceedings of the European Space Observatory conference on the power of optical/IR interferometry: recent scientific results and 2nd generation VLTI instrumentation at ESO, Garching bei Munchen 2005, “GENIE: a ground based European Nulling Instrument at ESO very large telecope interferometer.

[15] Cheng, Lun K., et al.: "Alternative fringe sensor for the DARWIN mission" SPIE 5905 (2005), 439

[16] Vosteen, L. L. A., et al.: "Darwin Infrared Nulling Interferometer Demonstrator" SPIE 5905 (2005), 102

[17] Labadie, Lucas, et al.: "Results on the development of mid-infrared integrated optics for the Darwin Mission" SPIE 5905 (2005), 80

[18] van den Dool, T. C., et al.: "The manufacturing, assembly and acceptance testing of the breadboard cryogenic Optical Delay Line for DARWIN" SPIE 5904 (2005), 367

[19] Cheng, Lun K., et al.: "Test results of the infrared single-mode fiber for the DARWIN mission" SPIE 5905 (2005), 442

[20] Cheng, Lun K., et al.: "Alternative fringe sensor for DARWIN mission" SPIE 5905 (2005), 434

[21] Ollivier, M.: "Darwin, un interferometre spatial pour observer les exoplanetes et y rechercher la vie" JPhy4 119 (2004), 73

[22] van den Dool, Teun C., et al.: "The design of a breadboard cryogenic optical delay line for DARWIN" SPIE 5528 (2004), 227

[23] Verlaan, Adrianus L., et al.: "TNO TPD contributions to high-precision optical metrology: a Darwin metrology breadboard for ESA" SPIE 5528 (2004), 32

[24] Labeque, Alain, et al.: "The Nulltimate project: building and testing, at low temperature achromatic phase shifters to prepare the Darwin mission" SPIE 5491 (2004), 999

[25] Brachet, Frank, et al.: "Nulling interferometry for the Darwin Mission: polychromatic laboratory test bench" SPIE 5491 (2004), 991

[26] Absil, Olivier; den Hartog, Roland H.; Gondoin, Philippe A.; Fabry, Pierre; D'Arcio, Luigi L.; Wilhelm, Rainer C.; Gitton, Philippe B.; Puech, Florence 2004, SPIE 5491,1257 ``Influence of atmosphericturbulence on the performance and design of GENIE".

[27] Gondoin, Philippe A.; Absil, Olivier; den Hartog, Roland H.; Wilhelm, Rainer C.; Gitton, Philippe B.; D'Arcio, Luigi L.; Fabry, Pierre; Puech, Florence; Fridlund, Malcolm C.; Schoeller, Markus; and 7 coauthors 2004, SPIE 5491, 775 ``Darwin-GENIE: a nulling instrument at the VLTI"

[28] den Hartog, Roland H.; Absil, Olivier; Gondoin, Philippe A.; D'Arcio, Luigi L.; Fabry, Pierre; Kaltenegger, Lisa; Wilhelm, Rainer C.; Gitton, Philippe B.; Puech, Florence; Fridlund, C. V. M. 2004, SPIE 5491, 160 ``The simulated detection of low-mass companions with GENIE"

[29] Kaltenegger, Lisa, et al.: "Requirements on the stellar rejection for the Darwin Mission" SPIE 5491 (2004), 275

[30] Fridlund, Malcolm C.: "Darwin and TPF: technology and prospects" SPIE 5491 (2004), 227

[31] Ergenzinger, Klaus, et al.: "FINCH: time-dependent simulation of nulling interferometry for the DARWIN mission" SPIE 5497 (2004), 226

[32] Beugnon, C et al.: "Design and modeling of the formation-flying GNC system for the DARWIN interferometer" SPIE 5497 (2004), 28

[33] van den Dool, Teun, et al.: "The design of a breadboard cryogenic optical delay line for DARWIN" SPIE 5495 (2004), 39

[34] Labèque, Alain, et al.: "New polychromatic testbed for DARWIN/TPF nulling interferometer laboratory demonstration" SPIE 4852 (2003), 405

[35] Fridlund, C. V. Malcolm, et al.: "Darwin mission" SPIE 4852 (2003), 394

[36] D'Arcio, Luigi, et al.: "The imaging mode of the infrared space interferometer IRSI-Darwin" SPIE 4852 (2003), 184

[37] Flatscher, Reinhold, et al.: "Nulling Breadboard for DARWIN" SPIE 4838 (2003), 712

[38] Gondoin, Philippe, et al.: "Darwin ground-based European nulling interferometer experiment (GENIE)" SPIE 4838 (2003), 700

[39] Gondoin, P.; Absil, O.; Fridlund, M.; Erd, C.; den Hartog, R.; Rando, N.; Glindemann, A.; Koehler, B.; Wilhelm, R.; Karlsson, A.; and 7 coauthors 2003, Proceedings of GENIE - DARWIN Workshop - Hunting for Planets (ESA SP-522). 3-6 June 2002. Leiden, The Netherlands. Editor: H. Lacoste. Published on CDROM., p.3.1 ``The Darwin Ground-based European Nulling Interferometry Experiment"

[40] Bakker, E. J.; Fridlund, M.; Gondoin, P.; Glindemann, A. 2003, Proceedings of GENIE - DARWIN Workshop - Hunting for Planets (ESA SP-522). 3-6 June 2002. Leiden, The Netherlands. Editor: H. Lacoste. Published on CDROM., p.1.1 ``Conference Executive Summary"

[41] Gondoin ,P.; Absil, O.; den Hartog, R.; Kaltenegger, L.; Eiroa, C.; Erd, C.; Fridlund, M.; Karlsson, A.; Peacock, A.; Sodnik, Z.; Volonte, S.; Wilhelm, R.; Schoeller, M.; Glindemann, A 2003, ESA SP proceedings of the Heidelberg conference ``Towards other Earth", p. 121 ``The Ground-based European Nulling Interferometry Experiment (DARWIN-GENIE)"

[42] Absil O., den Hartog R., Erd C., Gondoin P., Kaltenegger L., Fridlund M., Rando N., Wilhelm R., 2003, ESA SP proceedings of the Heidelberg conference ``Towards other Earth", p. 317 ``Geniesim: the GENIE simulation software"

[43] Absil O., Kaltenegger L., Eiroa C., den Hartog R., Gondoin P., Wilhelm R., Fridlund M., 2003, ESA SP proceedings of the Heidelberg conference ``Towards other Earth", p.323 ``Can GENIE characterize debris disks around nearby stars"

[44] den Hartog R., Absil O., Kaltenegger L., Gondoin P., Wilhelm R., Fridlund M., 2003, ESA SP proceedings of the Heidelberg conference ``Towards other Earth", p. 399 `` Could GENIE detect hot Jupiters"

[45] Kaltenegger L., Absil O., Eiroa C., Stankov A., Erd C., Gondoin P., den Hartog R., Fridlund M., Wilhelm R., 2003, ESA SP proceedings of the Heidelberg conference ``Towards other Earth", p. 465 `` Characterisation of disks around YSO's with GENIE"

[46] Haguenauer, Pierre, et al.: "Nulling interferometric breadboard using integrated optics beam combiners, preparation to the IRSI/DARWIN mission" SPIE 4838 (2003), 690

[47] Fridlund, C. V. Malcolm; Gondoin, Philippe 2003 SPIE 4852, 394, ``Darwin mission"

[48] Fridlund, M.; Gondoin, Ph. 2003, Astrophysics and Space Science, v. 286, Issue 1, p. 93-98 ``GENIE - The Darwin demonstrator"

[49] Gondoin, Philippe; Absil, Olivier; Fridlund, C. V. Malcolm; Erd, Christian; den Hartog, Roland H.; Rando, Nicola; Glindemann, Andreas; Koehler, Bertrand; Wilhelm, Rainer; Karlsson, Anders; and 7 coauthors 2003 SPIE 4878, 700 ``Darwin ground-based European nulling interferometer experiment (GENIE)"

[50] Absil, O.; Gondoin, P.; Erd, C.; Fridlund, M.; den Hartog, R.; Labadie, L.; Rando, N. 2003 Scientific Frontiers in Research on Extrasolar Planets, ASP Conference Series, Vol 294, Edited by Drake Deming and Sara Seager. (San Francisco: ASP) ISBN: 1-58381-141-9, 2003, pp. 557-560 ``Candidate VLTI Configurations for the GENIE Nulling Experiment"

[51] Gondoin, Ph.; Absil, O.; Erd, C.; Fridlund, M.; den Hartog, R.; Rando, N.2003, Hubble's Science Legacy: Future Optical/Ultraviolet Astronomy from Space, ASP Conference Proceedings, Vol. 291, held 2-5 April 2002 at University of Chicago, Chicago, Illinois, USA. Edited by Kenneth R. Sembach, J. Chris Blades, Garth D. Illingworth and Robert C. Kennicutt, Jr. ISBN: 1-58381-136-2, 2003., p.288 ``The Darwin-GENIE Experiment: An ESA-ESO Partnership"

[52] Haupt, Christoph, et al.: "High-precision optical metrology system for the SMART-2 mission as precursor for the DARWIN satellite constellation" SPIE 4777 (2002), 143

[53] Burger, J. F., et al.: "Vibration-free 5 K sorption cooler for ESA's Darwin mission" Cryo 42 (2002), 97

[54] Selsis, F., et al.: "Biomarkers and Tracers of Atmospheric Evolution of Exoplanets In The Spectroscopic Window of Darwin" EGSGA 27 (2002), 6058

[55] Ollivier, Marc, et al.: "Nulling interferometry for the DARWIN mission: experimental demonstration of the concept in the thermal infrared with high levels of rejection" SPIE 4006 (2000), 354

[56] Penny, Alan J., et al.: "DARWIN interferometer" SPIE 3350 (1998), 666

ESTEC
Keplerlaan 1 - NL 2201 AZ Noordwijk ZH - The Netherlands
Tel (31) - Fax (31) -

[57] Mariotti, Jean-Marie, et al.: "DARWIN infrared interferometer and the search for extra-solar life" SPIE 2477 (1995), 116

6.2 References related to Darwin Science

[58] Beaulieu, J-Ph., Bennet, D. et al, 2006, Nature, 439, 437

[59] Beichman, C., 2000, in Darwin and astronomy – The infrared space interferometer, ESA SP-451, 239

[60] Benedict, G.F., et al, 2002, Ap.J., 581, L115

[61] Bracewell, R.N., 1978, Nature, 274, 780

[62] Bracewell, R.N., McPhie, R.H., 1979, Icarus, 38, 136

[63] Butler, P., Marcy, G., 1996, Ap.J. Letters, 464, L153

[64] Charbonneau, D., Brown, T.M., Latham, D.W., Mayor, M., 2000, Ap.J., 529, L45

[65] Chelli, A., 2005, A & A, 441, 1205

[66] Dubovitsky, S., Lay, O.P., in Proceedings of SPIE, Volume 5491, p. 284

[67] Fridlund, M., 2000, ESA-SCI(2000)12

[68] Fridlund, M., et al, 2006, in preparation

[69] Hinz, P.M., Angel, J.R.P., Hoffman, W.F., McCarth et al. 1998, Nature, 395, 251

[70] Kaltenegger, L., Karlsson, A., 2004, in Proceedings of SPIE, Volume 5491, p. 275

[71] Stankov, A., Kaltenegger, L. et al, 2006 in preparation

[72] Latham, D.W., Stefanik, R.P., Mazeh, T. Mayor, M., Burki, G., 1989, Nature, 339, 38

[73] Le Coroller, H. et al, 2004 A & A, 426, 721

[74] Legér, A., Mariotti, J.M., Mennesson, B., Ollivier, M., et al, 1996a, Icarus, 123, 249

[75] Legér, A., Mariotti, J.M., Mennesson, B., Ollivier, M., et al, 1996b, Astrophysics & Space Sciences, 241, 135

[76] Mayor, M., Queloz, D., 1995, Nature, 378, 355

[77] Reuyl, D., Holmberg, E., 1943, Ap.J., 97, 41

[78] Sagan, C., 1980, in COSMOS, Random House Inc., ISBN 0-394-50294-9

[79] Selsis, F., 2002, In Proceedings of the First European Workshop on Exo-Astrobiology, 16 – 19 September 2002, Graz, Austria. Ed: Huguette Lacoste, ESA SP-518, Noordwijk, The Netherlands, p. 365

[80] Struve, O., 1952, The Observatory, 72, 199

[81] Traub, W., 2003, In Proceedings of the Conference on "Towards Other Earths: DARWIN/TPF and the Search for Extrasolar Terrestrial Planets, 22 – 25 April 2003, Heidelberg, Germany. Eds. M. Fridlund, T. Henning, complied by H. Lacoste. ESA SP-539, Noordwijk, The Netherlands: ESA Publications Division, p. 231

6.3 References related to Mission System Studies

[1] Lay, O.P., Applied Optics 43(33), 6100 (2004):

[2] Lay, O.P., *Removing Instability Noise in Nulling Interferometers*, Proc. SPIE 6268, pp. 62681A (2006)

[3] Chazelas, B., et al. Applied Optics 45 (5), 984 (2006)

[4] Lane, B., et al., *Calibrating an interferometric null,* ApJ 648, 1276 (2006)